# REPORT DOCUMENTATION PAGE

| 1. REPORT NUMBER | 2. GOVT A(  ON NO. | 3. RECIPIENT'S CATALOG NUMBER |
|---|---|---|
| )SR-T'          $\bigcirc$  /.) | | |

| 4. TITLE (and Subtitle) | 5. TYPE OF REPORT & PERIOD COVERED |
|---|---|
| SPREAD SPECTRUM MOBILE RADIO COMMUNICATION. | Final Report  'eb. 1, 1981 – Aug. 31, 1982 |
| | 6. PERFORMING ORG. REPORT NUMBER |

| AUTHOR(s) | 8. CONTRACT OR GRANT NUMBER(s) |
|---|---|
| S.C. Gupta | AFOSR 77-3277 |

| PERFORMING ORGANIZATION NAME AND ADDRESS | 10. PROGRAM ELEMENT. PROJECT, TASK AREA & WORK UNIT NUMBERS |
|---|---|
| Electrical Engineering Department Southern Methodist University Dallas, Texas 75275 | 2305 – B3    6110 2F |

| 11. CONTROLLING OFFICE NAME AND ADDRESS | 12. REPORT DATE |
|---|---|
| AFOSR/NE Building 410 | 12-31-82 |
| Bolling AFB, D.C. 20332 | 13. NUMBER OF PAGES  70 plus figures |

| 14. MONITORING AGENCY NAME & ADDRESS(if different from Controlling Office) | 15. SECURITY CLASS. (of this report) |
|---|---|
| As above in item 11. | unclassified |
| | 15a. DECLASSIFICATION/DOWNGRADING SCHEDULE |

16. DISTRIBUTION STATEMENT (of this Report)

Approved for public release;
distribution unlimited.

DTIC
ELECTE
APR 2   1983

E

17. DISTRIBUTION STATEMENT (of the abstract entered in Block 20, if different from Report)

19. KEY WORDS (Continue on reverse side if necessary and identify by block number)
Spread Spectrum, Mobile radio, Spectrum Efficiency, Rayleigh Fading,
Log-Normal Shadowing, Diversity Improvement, Adjacent Cell Interference

20. ABSTRACT (Continue on reverse side if necessary and identify by block number)
    In this report, we analyze the performance of frequency-hopped spread-spectrum systems under mobile radio channel conditions. Because of its good spectrum-efficiency, frequency-hopped systems seem to be natural candidates for mobile telephony in the near future. We analyze mainly the Frequency-Hopped-Multilevel Frequency Shift-Keyed (FH-MFSK) System, the reason being the established superiority of FH-MFSK over the other modulation, namely the Frequency-Hopped Differential Phase Shift Keyed system (FH-DPSK), under identical conditions.

DD FORM 1473  EDITION OF 1 NOV 65 IS OBSOLETE
1 JAN 73
S/N 0102-014-6601 |

83  04  20  234

Our new results include the spectrum efficiency analysis of FH-MFSK for various bandwidths of interest, the performance analysis of FH-MFSK under the influence of log-normal shadowing and Rayleigh fading, the possible performance improvement with the inclusion of a small number of space-diversity branches to combat the losses due to fading, a preliminary analysis of the occurence of burst errors in FH systems, the amount of degradation due to the users operating in the adjacent cells and a possible power control scheme to mitigate these effects and finally a result which establishes the near-equivalent performance of the hard-limited and the likelihood receivers under Rayleigh fading and multi-user interference conditions.

SPREAD SPECTRUM MOBILE RADIO COMMUNICATIONS

under contract

**AFOSR-TR- 83-0246**

AFOSR 77-32770

with

Air Force Office of Scientific Research
Bolling Air Force Base
Washington, D.C.

SCIENTIFIC REPORT

For the Period

February 1, 1981 –

August 31, 1982

S.C. GUPTA, PRINCIPAL INVESTIGATOR

# Electrical Engineering Department

# School of Engineering and Applied Science

## Southern Methodist University

Dallas, Texas 75275

SPREAD SPECTRUM MOBILE RADIO COMMUNICATIONS

under contract

AFOSR 77-3277

with

Air Force Office of Scientific Research

Bolling Air Force Base

Washington, D.C.

SCIENTIFIC REPORT

For the Period

February 1, 1981 -

August 31, 1982

Electrical Engineering Department

Southern Methodist University

Dallas, Texas 75275

Principal Investigator

S.C. Gupta

Professor and Chairman of Electrical Engineering

Phone (214-692-3113)

ATR

H (AFSC)

is

Ch. Information Division

Table of Contents

Summary

In this report, we analyze the performance of frequency-hopped spread-spectrum systems under mobile radio channel conditions. Because of its good spectrum-efficiency, Frequency-hopped systems seem to be natural candidates for mobile telephony in the near future. We analyze mainly the Frequency-Hopped-Multilevel Frequency Shift-Keyed (FH-MFSK) System, the reason being the established superiority of FH-MFSK over the other modulation, namely the Frequency Hopped Differential Phase Shift Keyed system (FH-DPSK), under identical conditions.

Our new results include the spectrum-efficiency analysis of FH-MFSK for various bandwidths of interest, the performance analysis of FH-MFSK under the influence of log-normal shadowing and Rayleigh fading, the possible performance improvement with the inclusion of a small number of space-diversity branches to combat the losses due to fading, a preliminary analysis of the occurence of burst errors in FH systems, the amount of degradation due to the users operating in the adjacent cells and a possible power control scheme to mitigate these effects and finally a result which establishes the near-equivalent performance of the hard-limited and the likelihood receivers under Rayleigh fading and multi-user interference conditions.

# CHAPTER I

## INTRODUCTION

This report summarizes new results on the performance of frequency-hopped spread-spectrum systems operating in mobile environment. The new results, which are arrived at after taking into consideration various real constraints imposed by mobile channel, are useful for the system designers. We have also proposed some modifications to improve the performance of these systems. In this chapter, we briefly review frequency-hopping systems for mobile radio. Subsequent chapters present our analysis and the results obtained from them.

## 1.1 Frequency-Hopped Spread Spectrum Systems for Mobile Radio:

The first attempt to introduce spread spectrum as a spectrally efficient scheme for mobile radio appeared with the proposal of a Frequency Hopped - Differential Phased Shift Keyed system (FH-DPSK) [1]. Generally, a direct sequence spread spectrum system performs very poorly under multi-user interference and fading channels. Frequency hopping (FH) schemes possess inherent capability to provide diversity against frequency-selective fading encountered in mobile channel. Henceforth, we shall consider only the FH schemes. Some of the advantages of the spread spectrum which are not easily achievable with other systems can be summarized.

1.  Inherent frequency diversity against fading as explained earlier. FM systems combat fading by increased transmitted power or space diversity or both.

2. All users can have access to the system any time [limited by equipment capacity]. There is no question of blocked cells as in channelized systems.

3. At times, increased user demand above the designed capability can be met by providing a 'gradual' degradation in the service quality to users rather than by denying services to certain users as in the other system. This aspect is important because the demand will exceed the design capacity during peak hours.

4. On the contrary, to item 3 above, priority requests can be met easily. For example, by increasing the output power to that user. This will ensure satisfactory service to the priority user.

5. Each user is assigned a unique address. This results in some grade of privacy.

6. Possibility of coexistence of both spread spectrum system and the conventional system, when full capacity of the spread spectrum is not needed.

Some disadvantageous features are: 1) power control is needed if FH systems are to operate in cellular radio; 2) equipment complexity is high both at the base station and at the mobile; 3) formidable technological problems in implementation and the questionable cost effectiveness.

An alternative to FH-DPSK is the Frequency Hopped Frequency Shift Keying (FH-FSK) and this has been shown to accomodate more simultaneous users than the former scheme. In the following paragraphs we shall discuss these two systems in some detail.

## 1-2  FH-DPSK System [1]

### A.  Transmitter

A block diagram of the FH-DPSK transmitter is shown in figure 1-1. There are two parts to the modulation process in the transmitter: addressing and encoding. Addressing is performed by the MFSK generator, which repeats with period T a specific sequence of N different tones or chips, each of duration $t_1$ ($t_1 = T/N$). The specific sequence is generated according to an assigned address to the user and each user is assigned an address which is distinguishable from others despite overlap in some positions. We shall look into some of the properties of the address set subsequently. Each mobile is fitted with a transmitter of the kind described and with a receiver to be described. The power radiated from each mobile is remotely controlled from the base station to ensure that all the signals arriving at the base station are nearly of equal strength. If this is not done, mobiles close to the base station will swamp the signals of those further away. This is the 'near-far' problem common to most spread spectrum systems.

Signal information is impressed or encoded onto the MFSK address sequence in the form of binary differential phase shift keying. If a binary-1 is to be transmitted in the $\ell^{th}$ chip of the address sequence, the phase of that chip is changed by $\pi$ radians relative to the phase in the $\ell^{th}$ chip of the previous sequence. For a binary +1, no phase change takes place. In order to increase the resistance of this type of modulation to interference, the allowed phase modulation sequences or words are selected from a set of N orthogonal words, such as the columns of Hadamard matrix. The Hadamard matrices are defined by:

$$H_2 = \begin{pmatrix} 1 & 1 \\ 1 & -1 \end{pmatrix} \qquad \text{1-1}$$

$$H_{2^n} = \begin{pmatrix} H_{2^{n-1}} & H_{2^{n-1}} \\ \\ H_{2^{n-1}} & -H_{2^{n-1}} \end{pmatrix} \qquad \text{1-2}$$

Any two rows (or any two columns) are orthogonal to each other. Or, in other words, any two rows agree pairwise in exactly half the num of portions and disagree in the rest. Which one of the N phase modulation sequences is used, is determined by the $\log_2 N$ signal bits at the input to the word buffer. Information rate can be seen as

$$R_b = \frac{\log_2 N}{T} = \frac{\log_2 N}{N t_1} \qquad \text{1-3}$$

B. Receiver

A block diagram of a typical receiver is shown in figure 1-2. There are N sections each with a band pass filter, delay element, product detector and a low pass filter. Each section is typical of a receiver used to detect DPSK signals [2]. The array of $t_1$ second delay lines and the set of N band pass filters selects the desired address waveform out of the incoming signal. In other words, the band pass filter center frequencies $(\omega_1 \ldots \omega_N)$ are uniquely related to the address of the user under consideration. Each band pass filter is matched to rectangular chip of duration $t_1$ and therefore, has a noise bandwidth of $1/t_1$. All N chips pass through the filters at the same time and their phases

(relative to the previous word) are detected using the T sec. delay
element and the product detectors. After low pass filtering to remove
the second harmonic product terms, the detector outputs are processed
in a combiner circuit. Different combining techniques yield different
performance. Linear combiner, which is implemented easily, also performs
poorly. Using likelihood combining, it is possible to improve the
performance significantly [3].

## Performance analysis of FH-DPSK system:

The maximum number of simultaneous users that could be accomodated
at a specific bit error rate is of interest in analyzing a digital mobile
radio system. Since this number could vary depending on the available band-
width or on the information bit rate, a measure defined as 'spectral
efficiency' is also useful:

$$\eta = \frac{M \; R_b}{W} \qquad\qquad 1\text{-}4$$

where $\eta$ is spectrum-efficiency, M is the number of users simultaneously
served by the system, $R_b$ is the bit rate per user and W is the one-way
bandwidth.

A comparison of average number of users per cell in a cellular
system for FH-DPSK and FM showed that they do not differ greatly [4].
As the above result was based on linear combining, further improvement
is possible with likelihood combiner. However it has been established
that a FH-MFSK system performs much better than the DPSK system under
identical conditions. i.e. FH-MFSK has a higher spectral efficiency $\eta$
for given values of $R_b$ and W.

## 1-3 Frequency-Hopping Multi-level Frequency-Shift Keyed System (FH-MFSK) [5]

A block diagram of the $m^{th}$ transmitter of FH-MFSK system is shown
in figure 1-3. Figure 1-4 shows the block diagram of the receiver.
The operation of the system can be understood by referring to these
figures. Every T seconds K message bits are loaded serially in a buffer
and transferred out as a K-bit word $X_m$. Assuming the modulo-$2^K$ adder
does nothing, for the moment, $X_m$ will select one of the $2^K$ possible
different frequencies from the tone generator. At the receiver, the
spectrum of each T second transmission is analyzed to determine which
frequency, and hence, which K-bit word, $X_n$ is sent. Of course, the
system as such is useless for multiple-user operation. If a second
transmitter were to generate $X_n$, neither the receiver m nor the receiver n
would know whether to detect $X_n$ or $X_m$. To avoid this, we add the address
generator as shown in figure 1-3 and assign a unique address to each user.

The basic interval T is divided into L intervals of duration $\tau$ each.
Over T seconds, the address generator of $m^{th}$ user generates a sequence of
L numbers:

$$a_m = (a_{m1}, a_{m2}, \ldots a_{mL}) \tag{1-5}$$

$$\text{Each } a_{mi} \,\epsilon\{0, 1, 2, \ldots 2^K - 1\} \tag{1-6}$$

Here, each $a_{mi}$ is selected at random from the set specified by 1-6 [called
'random address assignment'].

Now, each $a_{m\ell}$ is added modulo-$2^K$ to $X_m$ to produce a new K-bit number

$$Y_{m,\ell} = X_m + a_{m\ell}$$

or

$$\left. \begin{array}{l} \underline{Y} = (Y_{m1}, Y_{m2}, \ldots Y_{mL} \\[8pt] \underline{X}_m = (X_m, X_m, \ldots X_m) \\[8pt] \underline{Y} = \underline{X}_m + \underline{a}_m \end{array} \right\} \qquad 1\text{-}7$$

Each $\tau$ seconds, $Y_{m\ell}$ selects the corresponding transmitter frequency. At the receiver, demodulation and modulo $2^K$ subtraction by the same number $a_{m\ell}$ are performed every $\tau$ seconds, yielding

$$Z_{m\ell} = Y_{m\ell} - a_{m\ell} = X_m$$

The sequence of operations is illustrated by the matrices of figures 1-5a and 1-5b. Each matrix is either a sequence of K-bit numbers (code word, address, detection matrix) or a frequency-time spectrogram (transmit spectrum, receive spectrum). The matrices pertain to one link in a multi-user system. Crosses show numbers and frequencies generated in that link. Circles show the contributions of another link. As said earlier, the transmit spectrum is generated by modulating the address with code word using modulo-$2^K$ addition. Equivalently, when each entry in the address matrix is shifted cyclically by the row number specified by the code word matrix, we get the transmit spectrum 1-5a.

Because of multi-users, extraneous entries are created in the detection matrix. For example, a word $X_n$ transmitted over the $n^{th}$ link will be decoded by the receiver m as

$$Z'_{m\ell} = X_n + a_{n\ell} - a_{m\ell}.$$

-7-

The $Z'_{m\ell}$ are scattered over different rows. The desired transmission, on the other hand, is readily identified because it produces a complete row of entries in the detection matrix. Normally, the fading of the tones and the receiver noise can cause a tone to be detected when none has been transmitted (false alarm) and/or can cause a transmitted tone to be not detected (miss). Even without these impairments, many user entries can combine to produce a complete row other than $X_m$ and hence, can cause errors in the identification of correct row (in the word $X_m$). Hence, a majority logic rule is attempted: choose the code word associated with the row containing the greatest number of entries. Under this decision rule, an error will occur when insertions (detected tones due to other users and false alarms) combine to form a row with more entries than the row corresponding to the transmitted code word. An error can occur when insertions combine to form a row containing the same number of entries as the row corresponding to the transmitted code word. We view the transmission to each square in the tone detection matrix as an example of non-coherent on-off keying. Because of fading of amplitude and the random change of phase, it is not possible to employ coherent detection in mobile environment. (Recall that we used differential phase detection in FH-DPSK scheme, since the phase is not likely to change significantly from bit to bit).

From the text book formulas we have

$$P_F = \exp(-\beta^2/2) \qquad\qquad 1\text{-}8$$

$$P_D = 1 - \exp(-\beta^2/2(1+\bar{\rho})) \qquad\qquad 1\text{-}9$$

where $P_F$ denotes false alarm probability, $P_D$ the probability of deletion (miss), $\beta$ the normalized threshold set in the receiver and $\bar{\rho}$ the average

signal to noise ratio. The above scheme, where the presence or absence
of energy in each square of detection matrix is decided, together with
majority logic decision is called "Hard-limited Combining".

## Performance analysis - Hard limited receiver

We consider the transmission from base to mobiles in an isolated
cell mobile radio system. The delay spread in the arrival of waveforms
through different scatterers at a receiver varies from place to place, but
in any case remains less than few $\mu$ sec. on most occasions [6]. Since
typically $\tau \geq 13$ $\mu$ sec. in our system, as we shall see later, the delay
spread does not cause serious problems in achieving frame synchronization.
This is not the case with respect to mobile to base transmission, where
the propagation delay difference due to different vehicle locations make
synchronization very difficult. A typical non-coherent envelope analyzer
is shown in figure 1-6. Here, $r(t)$, the received waveform can be represented
as

$$r(t) = S_m(t) + \sum_{j=1}^{J} I_j(t) + n(t) \qquad 0 \leq t < T \qquad \text{1-10}$$

where $S_m(t)$ is the wanted signal at the $m^{th}$ receiver, $I_j(t)$'s are the
interferences due to J interferers and $n(t)$ is the white Gaussian receiver
noise. During the $\ell^{th}$ chip the waveforms can be represented as

$$S_m(t) = \alpha_{m\ell} \ A \sin(2\pi(f_o + \frac{b_{m\ell}}{\tau}) \ t + \phi_{m\ell}) \qquad \text{1-11}$$

$$I_j(t) = \alpha_{j\ell} \ A \sin(2\pi(f_o + \frac{b_{j\ell}}{\tau}) \ t + \phi_{j\ell}) \qquad \text{1-12}$$

-9-

Here, $b_{m\ell} = (X_m + a_{m\ell}) \bmod 2^K$, $\alpha_{m\ell}$, $\alpha_{j\ell}$ are Rayleigh distributed with $E(\alpha_{m\ell}^2) = E(\alpha_{j\ell}^2) = 1$, $\phi_{m\ell}$, $\phi_{j\ell}$ are uniformly distributed over $(0, 2\pi)$. Thus, we assumed the envelope to be Rayleigh distributed and neglected the shadow fading effects. By comparing $R_{n\ell}$ against some threshold T we declare whether energy is present in the $n^{th}$ envelope detector during $\ell^{th}$ chip. The procedure is done for all $n = 0, 1, 2, \ldots 2^K-1$ and repeated for every $\ell = 1, 2, \ldots L$. Thus, an entry $(n, \ell)$ is created in the received matrix

if $\quad R_{n\ell} > T$

or $\quad \left[ R_{n\ell} \bigg/ \sqrt{N_o/2} \right]^2 > \left[ T \bigg/ \sqrt{N_o/2} \right]^2 = \beta^2$ $\qquad$ 1-13

where $N_o/2$ is the two-sided power spectral density of noise. Because of noise $n(t)$ and interferences $I_j(t)$ spurious entries occur in the received matrix. The probabilities

$$P_D = \text{Prob} \ [R_{n\ell} < T \cdot | \ b_{m\ell} = n] \ \text{and} \ P_F = \text{Prob}[R_{n\ell} > T | b_{m\ell} \neq n]$$

can be easily calculated and the results were mentioned earlier in 1-8 and 1-9.

Once the signal-to-noise ratio $\bar{\rho}$ and $\beta$ are fixed, the average $P_D$ and $P_F$ [why these are called 'average values' and how these can be used to have a realistic estimate under selective fading is explained well in the appendix of [5]] can be computed. Since the $2^K$ tones span the entire bandwidth and each occupy approximately $1/\tau$ Hz, we have

$$W = 2^K/\tau \qquad\qquad 1-14$$

Thus, the spacing of tones at $1/\tau$ ensures approximate orthogonality of tones. Also, the bit rate $R_b$ of a user is related to other parameters by

$$R_b = \frac{K}{L\tau} \qquad\qquad 1\text{-}15$$

Since W and $R_b$ are fixed (W by the FCC spectrum allocation and $R_b$ by the specific speech coding or if it were data, by the data rate) we have only one parameter (K or L) to choose at our will. Typical values of these parameters are shown in the following table I.

Table I

| W = 20 MHz | | |
| --- | --- | --- |
| $R_b$ = 32 K bit/sec. | | |
| K | L (Largest integer) | $\tau$ $\mu$ sec. |
| 6 | 58 | 3.2 |
| 7 | 34 | 6.14 |
| 8 | 19 | 11.63 |
| 9 | 10 | 23.26 |

With M = J + 1, the number of users served by the system, it is possible to compute $P_b$ as a function of M and K by using a set of formulae derived for the hard-limited receiver in [5]. Except when the signal-to-noise ratio $\bar{\rho}$ is very low, which then necessitates higher number of diversity (i.e. large L and low K), for all the other cases K = 8 is found optimum. i.e. it supports maximum number of users at a bit error rate $P_b < 10^{-3}$. With 32 K bit ADM speech, a $P_b$ of $10^{-3}$ could result in a good intelligible speech. The results of this analysis are shown in 1-7.

Because of its superior performance, we considered only the FH-MFSK system in our analysis. As one can observe, the results obtained earlier assumed a simplified mobile radio model. For example, the effect of log-normal shadowing was neglected in the analysis. Also, only isolated cell was considered. In a realistic cellular system, the adjacent cells could interfere significantly and degrade the performance. Some power control scheme is required for reducing the adjacent cell interference. All these problems were considered in our analysis. We present our analysis and the results in the following chapters.

II.  Spectrum Efficiency of FH-MFSK under Rayleigh Fading for Different
     Bandwidths

Here, the spectrum efficiency of a frequency-hopped multilevel

shift keying (FH-MFSK) spread spectrum modulation technique proposed

for use in mobile radio systems is evaluated.  The analysis assumes

randomly chosen address vectors, a perfect synchronization at the reciever,

and noncoherent detection.

With perfect transmission where the only degradation is due to

mutual interference, the efficiency is 0.262, 0.295 and 0.345 at an

average bit error rate of $10^{-3}$ for 1.64, 3.41 and 20 MHz bandwidth.

However, with transmission impairments consisting of additive white

Gaussian noise and frequency selective Rayleigh fading, which characterizes

the mobile radio channel, the efficiency depends on the average signal-

to-noise ratio, and on the average bit error rate. [7]

Assuming a random address vector, Goodman [5], derived a set of

formulas which give the upper bound on the average bit error rate

(see appendix 2-1). The system performance depends on, message block

size K, number of users M, the available bandwidth W, and the average

signal to noise ratio $\gamma_0$.

2-1  Spectrum Efficiency Analysis

    a.  Rayleigh fading with additive white Gaussian noise:

In this paper we assume that the transmission to each square in

the received matrix as noncoherent on-off keying.  The probability of

false alarm, $P_F$, and the probability of average miss, $P_D$, are given by

$$P_F = \exp\left(-\frac{b^2}{2}\right) \qquad\qquad 2\text{-}1$$

$$P_D = 1 - \exp\left[-\frac{b^2}{2(1+\gamma_0)}\right] \qquad\qquad 2\text{-}2$$

where $\gamma_0$ is the average signal-to-noise ratio, and b is the normalized detection threshold. In this analysis we choose the optimum value of b, $b_0$ which minimizes the overall probability of error.

$$b_0 = \sqrt{2\left(1 + \frac{1}{\gamma_0}\right) \ln(1 + \gamma_0)} \qquad\qquad 2\text{-}3$$

The required bandwidth for the system, with the doppler shift ignored is given by

$$W = \frac{2^K L R}{K} \qquad\qquad 2\text{-}4$$

where R is the data rate, bits per second, assumed to be fixed in the analysis as 32 K bit/sec, L the number of chips, and K is the message block size. The analysis considers three values of W: 1.64, 3.41 and 20 MHz. For each value of W and $\gamma_0$, $(\hat{K},\hat{L})$ the optimum value of (K,L), which maximize the number of users M, whom can be served simultaneously by the system at an average bit error rate $P_B = 10^{-3}$, is estimated by using the search method along with eq. 2-1 – 2-4 and the set of formulas in appendix 2-1. Figs. 2-1, 2-2, and 2-3 show the value of (k,L) and M for $\gamma =$ 25, 30 and 35 dB, for W = 1.64, 3.41 and 20 MHz respectively.

The spectrum efficiency of the system as a function of bandwidth with average bit error rate $P_B$ and SNR as parameters, is evaluated using the values of $(\hat{K},\hat{L})$ along with eq. 2-1, 2-2 and 2-3 and the set of formulas in Appendix 2-1. The result is shown in Figure 2-4.

b. Noiseless Case

In the absence of noise, the only degradation in the system performance is due to the mutual interference between the users. It can be shown that the upper bound on the average bit error rate is given by

$$P_B \leq 2^{K-2} P^L \qquad\qquad 2\text{-}5$$

where

$$P = 1 - (1 - 2^{-K})^{M-1} \qquad\qquad 2\text{-}6$$

By search methods, and using 2-4, 2-5, and 2-6, $(\hat{K}, \hat{L})$ and $\hat{M}$ can be estimated for a particular value of W and an acceptable average bit error rate $P_B = 10^{-3}$, Figs. 2-1, 2-2, and 2-3 show the values of K, L and M for $\gamma_0 = \infty$ (noiseless) and W = 1.64, 3.41, and 20 MHz, respectively. Figure 2-4 shows the spectrum efficiency as a function of bandwidth for $\gamma_0 = \infty$ and the average bit error rate $P_B$ as a parameter.

## 2-2 Conclusion

In this paper the spectrum efficiency of the frequency-hopped multi-level frequency-shift keying system has been evaluated taking into consideration white Gaussian noise and frequency-selective Rayleigh fading with $\gamma_0$ and $P_B$ as parameters, assuming a randomly chosen address vector.

The capacity of the system M is increased as the bandwidth is increased as seen from figures 2-4, 2-5 and 2-6. Hence, this suggests that the splitting of bandwidth into smaller blocks is not useful. As a comparison at $P_B = 10^{-3}$, SNR = 25 dB and W = 20 MHz, the spectrum efficiency $\eta$ for FH-DPSK equals 0.025 [4]. Whereas for FH-MFSK, $\eta = 0.272$. This confirms that FH-MFSK has better performance than FH-DPSK under identical conditions.

## Appendix 2-1

Probability of insertion due to interference

$$P = [1-(1-2^{-K})^{M-1}] \; (1-P_D)$$

Probability of insertion due to interference and false alarm

$$P_I = P + P_F - PP_F$$

Probability of m entries in spurious row

$$P_s(m) = \begin{pmatrix} L \\ m \end{pmatrix} \; P_I{}^m (1-P_I)^{L-m}$$

Probability that no unwanted row has as many as n entries

$$P(n,o) = \left( \sum_{m=0}^{n-1} P_S(m) \right)^{2^K-1}, \text{ for } n > 0$$

Probability that n is the maximum number of entries in an unwanted row and only one unwanted row has n entries.

$$P(n,1) = (2^K-1) \; P_s(n) \; \left( \sum_{m=0}^{n-1} P_s(m) \right)^{2^K-2} \quad n = 1, 2, \ldots, L$$

Probability of i entries in the correct row

$$P_c(i) = \begin{pmatrix} L \\ i \end{pmatrix} \; (1-P_D)^i \; P_D{}^{L-i}$$

Upper bound on average bit error rate

$$P_B \le \frac{2^{K-1}}{2^K-1} \left( 1 - \sum_{i=1}^{L} P_c(i) \; [P(i,o) + \tfrac{1}{2} P(i,1)] \right)$$

-17-

III. Performance of FH-MFSK System under Rayleigh Fading and Log-Normal Shadowing

We evaluate the performance of the system by studying the bit error probability caused aby transmission impairments. Here, the degradation in system performance due to a Rayleigh fading and log-normal shadowing environment is evaluated. [8]

With perfect transmission where the only degradation is due to mutual interference, the system can accommodate up to 209 simultaneous users at an average bit error rate of $10^{-3}$. However, with frequency selective Rayleigh fading and log-normal shadowing with standard deviation of 6 dB and normalized area mean of 20 dB the system can accomodate only up to 110 simultaneous users at the same error rate.

## 3-1  Introduction

In mobile radio environment the received signal envelope, S fluctuates rapidly due to multipath propagation and wave interference, the signal envelope has a Rayleigh probability density function (Rayleigh fading). The local mean of the Rayleigh distributed signal envelope is fairly constant over distances of a few tens of wave lengths, as a mobile moves over a large distance the local mean varies due to the terrain and the effect of other obstacles. [6]

In this paper the effect of Rayleigh fading and log-normal shadowing on the performance and on the spectrum efficiency of frequency-hopped multilevel-FSK spread-spectrum are evaluated.

Spectrum efficiency is measured by the number of bits per second per unit of the bandwidth, i.e. if M is the number of the users served by the system simultaneously, W is the one way bandwidth and R is the data rate then the spectrum efficiency $\eta$ is

$$\eta = \frac{MR}{W}$$

3-2 **Performance of on-off keying system with noncoherent detection in Rayleigh fading and lognormal shadowing**

The conditional false alarm probability $P_{f\gamma}$, and conditional miss probability $P_{d\gamma}$ due to additive white Gaussian noise with one sided power spectrum density N are [9]

$$P_{d\gamma} = 1 - Q(\sqrt{2\gamma}, \, \beta_o) \qquad\qquad 3-1$$

$$P_{f\gamma} = \exp\left(-\frac{\beta_o^2}{2}\right) \qquad\qquad 3-2$$

where, $\beta_o$ is the normalized threshold level $\beta/\sqrt{N}$

$\gamma$ is the signal to noise ratio $\quad S^2/2N$

and $Q(a,b)$ is the Q-function

With Rayleigh fading and lognormal shadowing the signal envelope S, has a probability density function [10]

$$P(S) = \sqrt{\frac{\pi}{8\sigma^2}} \int_{-\infty}^{\infty} \frac{S}{10^{\overline{S}_d/10}} \exp\left(\frac{-\pi S^2}{4 \times 10^{\overline{S}_d/10}}\right) \exp\left(-\frac{(\overline{S}_d - m_d)^2}{2\sigma^2}\right) d\overline{S}_d$$

where, $\overline{S}_d$ is the mean of Rayleigh distribution in dB, i.e. $\overline{S}_d = 20 \log_{10} \overline{S}$, $\overline{S} = <S>$.

$m_d = <\overline{S}_d>$ and $\sigma$ (typically 6 to 12 dB in urban areas), are the mean and standard deviation of the lognormal shadowing.

The mean-square value of Rayleigh distribution is $4\bar{S}^2/\pi$. By a simple random variable transformation the probability density function of signal to noise ratio $\gamma = S^2/2N$, is given by

$$P(\gamma) = \frac{10}{\log_e 10 \; \sqrt{2\pi\sigma^2}} \int_0^\infty \frac{1}{\gamma_0^2} \; \exp(-\frac{\gamma}{\gamma_0}) \; \exp\left[-\frac{1}{2\sigma^2}(10\,\log_{10}\frac{\gamma_0}{\bar{m}_d})^2\right] d\gamma_0 \qquad 3$$

Where, $\gamma_0 = 4\,\bar{S}^2/2\pi N$ is the mean signal to noise ratio over Rayleigh fading. And $\bar{m}_d = 4 \times 10^{m_d/10}/2\pi N$ is the normalized area mean with respect to noise power spectrum density N.

The probability of error $P_F$ and $P_D$ is obtained by averaging $P_{f\gamma}$ and $P_{d\gamma}$ over $\gamma$, i.e.

$$P_D = \int_0^\infty P_{d\gamma} \; P(\gamma) \; d\gamma$$

$$= 1 - \frac{1}{\sqrt{2\pi}} \int_{-\infty}^\infty \exp\left[-\frac{\beta_0^2}{2(1+\bar{m}_d \, 10^{\sigma x/10})}\right] \exp\left(\frac{-x^2}{2}\right) dx \qquad 3\text{-}5$$

$$P_F = \int_0^\infty P_{f\gamma} \; P(\gamma) \; d\gamma$$

$$= \exp\left[-\frac{\beta_0^2}{2}\right] \qquad 3\text{-}6$$

For $\sigma = 0$ (no shadowing) the p.d.f. of S is simply a Rayleigh distribution with a mean $m_d$ in dB, i.e. $\gamma_0 = \bar{m}_d$ thus eq. 3-5 becomes

$$P_D = 1 - \exp\left[-\frac{\beta_0^2}{2(1+\gamma_0)}\right] \qquad 3\text{-}7$$

and $P_F = \exp\left[-\frac{\beta_0^2}{2}\right]$ \qquad 3\text{-}8

## 3-3  System Performance and Spectrum Efficiency Analysis

The average bit probability of error $P_B$ is a function of, the number of chips L, message block size K, false alarm probability $P_F$, miss probability $P_D$ and the number of simultaneous users served by the system M, see appendix 1 of chapter 2.

The optimum $\hat{K}$, $\hat{L}$ which maximizes M can be obtained by a search method for a specified value of $P_B$, $P_F$, $P_D$ and W.  It has been shown [5] that $\hat{K}$, $\hat{L}$ depends weakly on $P_D$ and $P_F$.  For an acceptable error rate $P_B = 10^{-3}$, and specified bandwidth of 20 MHz the optimum value of K and L are 8 and 19 respectively.

The values of $\hat{K} = 8$ and $\hat{L} = 19$, with the set of equations in appendix 1 of chapter II are used to compute the constant M contours by using (Newton – Rapshun method) for $P_B = 10^{-3}$, broken line in fig. 3-1.  Each curve is a contour of false alarm probability $P_F$ and miss probability $P_D$, for constant M.

The integral in eq. 3-9 has been evaluated numerically, together with eqs. 3-6 and 3-7 the receiver  operating curves can be computed, solid line in fig. 3-1 for $\sigma = 0$, 6 and 12 dB respectively.  The normalized area mean $\overline{m}_d$ and normalized threshold $\beta_0$ are taken as a parameter.

The system performance, the maximum number of simultaneous users the system can accommodate at a given normalized area mean and standard deviation, can be evaluated by locating the tangent point of constant M contour curve and receiver operating curve.

For $\overline{m}_d = 30$ dB the system can accommodate 192 and 130 simultaneous users at an average bit error rate less than $10^{-3}$ for $\sigma = 0$ (fading only) and $\sigma = 12$ dB (worst case of shadowing) respectively, that is a reduction

of 8% and 38% from the system capacity for a perfect transmission. Also, the optimum value of normalized threshold (which minimizes the probability of error $P_B$) can be obtained directly from the curve for specific $\overline{m}_d$ and $\sigma$.

Using the values of $P_D$ and $P_F$ which maximize the number of users (tangent points at fig. 3-1) to calculate the average probability of error $P_B$ for a certain value of M, together with equation1, the spectrum efficiency of the system can be evaluated. Fig. 3-2 shows the spectrum efficiency verses the average probability of error for W = 20 MHz and $\sigma$ = 0, 6, 12 dB shadowing standard deviation respectively and $\overline{m}_d$ taken as a parameter.

## Conclusion

The spectrum efficiency and system performance for Frequency-Hopped Multilevel FSK has been calculated for the realistic mobile radio case, with lognormal shadowing is directly proportional to the distance between mobile unit and the base station.

The results show that the system capacity decreases to 130 users for $\overline{m}_d$ = 30 dB, and $\sigma$ = 12 dB at an average bit error rate of $10^{-3}$, that is 38% degradation from a perfect transmission.

The spectrum efficiency of the system also decreases as standard deviation and normalized area mean increase, for example, for $\overline{m}_d$ = 30 dB the spectrum efficiency will vary from 0.231 to 0.312 bits per second per unit of bandwidth, as $\sigma$ varies from 12 to 0 dB.

IV. Burst Error Analysis of FH Systems for Mobile Radio

Here, we analyze the occurence of burst errors in FH systems from a statistical point of view, making some crude but reasonable assumptions [17]. The results for synchronous transmission from base to mobiles indicate that in FH-DPSK errors occur mostly randomly, whereas in FH-MFSK the burst errors are likely to be significant in some suburban areas where correlation bandwidths exceed 0.8 MHz.

4-1  Introduction

In earlier analyses of FH systems, an average probability of bit error of $10^{-3}$ is assumed as the criterion for good speech quality. However, it is observed in conventional FM systems that as the vehicle moves through fading signal pattern, capture effect produces interruption during this period. The interruptions have different subjective quality (producing clicks) depending on vehicle speed [11]. In data transmission, these interruptions produce burst of errors, creating need for additional redundancy. Here, we give an approximate analysis of burst error statistics for these FH systems. It will be observed that the FH-DPSK system experiences essentially only random errors and hence, the criterion of average probability of bit error of $10^{-3}$ is adequate to provide good speech quality. Same conclusion could not be arrived at for FH-FSK system. However, for data transmission and signalling additional redundancy techniques would be required, in either system.

-23-

4-2   Burst Error Analysis of FH-FSK System

Consider the FH- multilevel FSK system.  We will restrict
our attention to synchronous transmission from base to mobile units,
assuming perfect synchronization at the receiver.  A number of tones
arriving at the mobile may be 'lost' during deep fades, resulting in
'deletion error'.  The number of tones that would fade simultaneously
depend on the correlation bandwidth $\Delta$ of the channel.  Here correlation
bandwidth is defined with respect to a correlation coefficient of 0.9.
Usually, $\Delta$ varies from > 0.04 MHz in urban areas to > 0.25 MHz, < 1 MHz
in suburban areas [12].  Whereas, when some of the tones of wanted
signal at the receiver fade, it is possible that some tones of the
interferring signals also fade at the same time.  This, in effect,
increases the average probability of deletion during $p_{DF}$ and ultimately
the probability of word error during fade $p_{WF}$.

During the period of deep fades probability of a tone being in
fade bandwidth is

$$p = \frac{\Delta}{20} \quad , \quad \text{assuming 20 MHz one way bandwidth}$$

Here we make an assumption that the fade bandwidth is the same as
correlation bandwidth.  i.e. two tones separated in frequency by no greater
than the correlation bandwidth would fade together.  Then, assuming
random selection of tones, probability of finding x tones in the fade
bandwidth follows binomial distribution.

Given that at least one tone fades during certain period, probability that x tones fade simultaneously is

$$P[X = x \mid X \geq 1] = \frac{p[X = x, X \geq 1]}{p[X \geq 1]}$$

$$= \begin{cases} \dfrac{P_x}{\displaystyle\sum_{x=1}^{L} P_x} & x \geq 1 \\[6pt] 0 & x = 0 \end{cases}$$

where
$$P_x = \binom{L}{x} p^x (1 - p)^{L-x} \qquad\qquad 4\text{-}1$$

L = number of tones per word from any user.

We assume here that fading refers to the situation when the envelope goes below the threshold β set in the receiver which detects the ON/OFF keyed tones.

Whenever a tone falls in the fade bandwidth, it will not be detected at the mobile and, hence, a 'deletion error' occurs. An average probability of deletion during fade can be defined as

$$P_{DF} = \frac{\text{Expected number of tones deleted during fade}}{\text{Total number of tones transmitted}}$$

$$= \frac{1}{L} \cdot \sum_{x=1}^{L} \frac{x P_x}{\left( \displaystyle\sum_{x=1}^{L} P_x \right)}$$

-25-

$$P_{DF} = \frac{p}{[1-(1-p)^L]} \qquad\qquad 4\text{-}2$$

When the correlation bandwidth is high, as in some suburban areas, it is possible that more than few tones would fade together. Hence, in general, we can define the conditional probabilities

$$P(X=x \mid X \geq J) \qquad \text{and hence an average } p_{DF} \text{ during fade as}$$

$$P_{DF} = \frac{E[X \mid X \geq J)]}{L} \qquad\qquad 4\text{-}3$$

The value that J would assume depends on $\Delta$. For $\Delta < 0.2$, the probability that $P(X \geq 2)$ is too low (less than 2%) and hence $p_{DF}$ can be assumed to be as given in 4-2. For $\Delta > 0.8$, the probability that $P(X \geq 2)$ is still high and hence the following expression for $p_{DF}$ is reasonable.

$$P_{DF} = \frac{E[X \mid X \geq 2]}{L} \qquad\qquad 4\text{-}4$$

In practice for $\Delta > 0.8$ we can expect the value of $p_{DF}$ to be somewhere between the values in 4-2 and 4-4, on most occassions.

Then it is possible to calculate the average probability of bit error $P_{bF}$ as discussed in [5] but with $p_{DF}$ as the probability of deletion. $p_F$ does not change since it depends only on $\beta$ and not on the signal statistics.

Results obtained with SNR of 25 db ($\beta = 2.75$) are shown in Fig. 4-1 for the cases $\Delta = 0.2$, and 1 MHz. Also shown is the average error curve from [5]. The figure shows that during fading the bit error rate is expected to be significantly larger than the average error rate.

## Fading Statistics:

The duration and recurrency of fades depend on the vehicle speed and on the threshold used in the definition of fade. The threshold of $\beta = 2.75$ at SNR of 25 db represents a level of 18 db below the mean value of the signal. For this threshold and at 850 Mhz, we can get the fading statistics from [12, 13]. They are reproduced in Table I along with expected number of bits in error E(N), during fading.

| V miles/hr. | $\tau_f$ m sec. | N | E(N) $= N \times P_{bF}$ $P_{DF}$ from (2) | E(N) $= N \times P_{bF}$ $P_{DF}$ from (4) |
|---|---|---|---|---|
| 1 | 34.66 | 1,109 | 37 | 77 |
| 4 | 8.67 | 277 | 9 | 19 |
| 20 | 1.73 | 55 | 2 | 3 |
| 70 | .49 | 15 | - | 1 |

Table I

$\Delta$ = 1 MHz

M = Number of users = 170

$\tau_f$ = fade duration

N = Number of bits contained in fade duration, with 32 k bs data rate

E(N) = Expected number of bits in error during $\tau_f$

## 4-3 Burst Error Analysis of FH-DPSK System

We consider the FH-DPSK system [1,14]. As before, synchronous transmission from base to mobiles is assumed. Unlike in FH-FSK scheme with perfect synchronization and orthogonality of tones, there will be no interference from other users and, hence, the system capacity is not limited by interference. We follow the approach in [14] for this analysis.

Probability of bit error $P_{bF}$ is bounded by

$$\frac{N}{2(N-1)} \; P_p \leq P_{bF} \leq \frac{N}{2} \; P_p$$

where

$P_p$ = Error probability of pairwise comparison

N = Number of code words = Number of transmitted tones, taken to be 32 here.

The only difference between the analysis in [14] and here is that during fading the random variables $\phi_i$'s are not independent. Only $L = N/2$ tones out of a total of N transmitted tones affect $P_p$. We assume an approximate model in that $N_1$ tones out of L fade together whereas the remaining $(L - N_1)$ tones experience no fading (flat fading). Then, the probability density of $(\phi_1 \ldots \phi_L)$ is given by

$$p(\phi_1 \ldots \phi_L) = \prod_{j=1}^{N_2} \delta(\phi_j - 1) \; \prod_{k=1}^{N_1} \delta(\phi_k)$$

and $N_1 + N_2 = L$

Proceeding as in [14], $P_p$ can be found to be

$$P_p = \frac{1}{2\pi i} \int_c (1 + z^2)^{-L} \exp \left( i \left( \frac{Z \cap N_2}{1 - iZ} \right) \right) \; \frac{dZ}{Z}$$

-28-

Where c is the real axis except for an indention above the origin.

Evaluating the above, we get

$$P_p = \exp\left[-\frac{N_2\rho}{2}\right] \sum_{\ell=0}^{L-1} \sum_{n=\ell}^{L-1} 2^{-L-n} \binom{L-1+n}{n-\ell} \frac{\left(\frac{N_2\rho}{2}\right)^{\ell}}{\ell!} \qquad 4\text{-}5$$

Using the results in Section II with an average $P_{DF}$, we get an average value for $N_1$ as

$$N_1 = L\, P_{DF}$$

For $\Delta = 1$ MHz, $L = 16$, $N_1$ is approximately 2 and, hence, $N_2 \approx 14$. This indicates @ $E_b/N_0 = 10$ db, $P_{bF} \leq 0.59 \times 10^{-4}$ which is very low compared to $P_{bF}$ of FH-FSK at $\Delta = 1$ MHz.

## 4-4  Discussion and Conclusion:

It is seen that FH-DPSK performs better than FH-FSK since the $P_{bF}$ for the former is low even with high correlation bandwidth of 1 MHz. The analysis is greatly simplified in that only base to mobile transmission with perfect synchronization is considered.  A rigorous analysis should yield the cumulative distribution function of average burst error lengths. Shadow fading will affect the average number of possible users at an average bit error rate of $10^{-3}$ but will not essentially change the burst error statistics.

## V. Diversity Improvement in Frequency Hopping Multilevel FSK Systems Under the Influence of Rayleigh Fading and Log-normal Shadowing

While the advantage of the inherent frequency diversity against fading is well-known, the improvement in the system performance due to the use of space diversity has not been studied. Here, we analyze the performance of FH-MFSK under the influence of Rayleigh fading and log-normal shadowing due to the combined use of frequency and space diversities. [15]

It is shown by analysis that the system capacity can be increased from the corresponding non diversity figure by 26.3% relative to the full system capacity (i.e. 209 users) with the use of diversity branches at channel condition of 10 dB normalized area mean and worst case of shadowing $\sigma = 12$ dB.

Also, graphical results are given for different channel environments, and required signal to noise ratio.

### 5-1 Introduction

It is well-known that the extreme and rapid signal variations associated with the mobile radio transmission path will increase the bit error rate, hence drastically reducing the system capacity. Diversity combining is used to reduce the signal variations to a range that will improve reliability in the system reception and permit acceptable transmission of voice. Diversity is accomplished by making N identical transmission paths all carrying the same message but having statistically independent time fluctuations. It is assumed that the mean signal strength of each transmission path is approximately

the same. A variety of techniques has evolved for combining the signals from these transmission paths at the receiver site. In this paper we will assume an equal-gain combining of the appropriate energy detector outputs. Maximal ratio combining can be used instead of equal-gain combining; in this method (maximal ratio combining) each energy detector is weighted proportionally to the signal to noise power ratio and then summed. It has been shown [6]

Here, it is shown that the system capacity can be drastically increased with the use of small number of space diversity branches. At microwave frequencies, space diversity can be achieved at the mobile unit with antenna spacing on the order of one-half wavelength or larger [6]. However, since most of the scatterers in the mobile-base transmission path are in the vicinity of the mobile unit, spacing on the order of tens of wavelengths is needed at the base station to achieve space diversity. The • diversity array can be located either at the mobile unit, the base station, or both, also there is no limitation on N the number of diversity branches. However, the system complexity increases linearly with N, but the relative improvement decreases as N grows larger.

Variations in signal level with time are caused by multipath wave interference. It is well-known that the signal envelope seen by a mobile radio antenna has a Rayleigh distribution with a fairly constant local mean over a small area. However, as the vehicle moves in the service area the local mean varies due to changing in the topographical area surrounding the mobile unit. Based on experimental evidence, it has been shown that the local mean signal envelope (the mean of Rayleigh distribution can be approximated by a log-normal distribution with area mean $m_d$, and standard deviation $\sigma$ as parameters. The channel mathematical model assumed in this paper is Rayleigh fading and log-normal shadowing.

## 5-2  Description of Transmitter and Receiver

The transmitter of a FH-MFSK system can be described in terms of a block diagram, fig. 5-1. Each user is assigned an L words address vector $a_m$ with each word having K bits. Every T second the transmitter collects K successive bits generated at a rate of D bits/second (assumed to be 32 K bit/sec.) in a register and transfers it as a K bit word $X_m$ to the buffer. The data word $X_m$ is used to modulate the address by modulo $2^K$ addition and, hence, produce a new sequence $C_m$ of length L, each $C_{m\ell}$ being of T/L seconds duration. The new formed sequence $C_m$ is used to select L tones from $J = 2^K$ orthogonal frequencies available from the tone generator.

The receiver implementation consists of a frequency dehopper and N x J energy detectors, fig. 5-2. Each energy detector consists of a bandpass matched filter followed by a square-law envelope detector. The corresponding (one of the J) energy detector outputs $Y_{in\ell}$ from each (of the N) diversity channels are linearly summed (equal gain combining) i.e. $R_{n\ell} = \sum_{i=1}^{N} Y_{in\ell}$. The outputs of the J summers $R_{n\ell}$ are then periodically sampled at a rate of $\tau = T/L$ seconds and then compared against a threshold. The majority logic receiver chooses the word $\hat{X}_m$ corresponding to the largest $\hat{Z}_n$ where $\hat{Z}_n = \sum_{\ell=1}^{L} \hat{R}_{n\ell}$. Mutual interference, multipath propagation and AWGN give rise to a detection error. This is because of the tones from other users and false alarms (a tone can be detected when none has been transmitted due to noise and propagation conditions) combine to form a row having higher sum than $\hat{Z}_m = \max_n \hat{Z}_n$. Goodman et. al. [5] derived a set of formulas which give the upper bound on the average bit error rate as a function false alarm $P_F$, miss probability $P_D$, message block size K, number of users M and the available bandwidth W (see appendix I). Throughout the analysis a perfect synchronization between mobile and its base station is assumed, also the address sequence $a_m$ of each user is chosen at random.

We will assume that the signal envelope on each of the diversity channel is independently perturbed by Rayleigh fading, log-normal shadowing, and AWGN which has the same r.m.s. value $N_0$ in each channel. This is a reasonable assumption because the antenna separation at the mobile unit is larger than one-half of the wavelength. Noncoherent or envelope detection is used since information about the phase of the received signal is not available at the receiver. Under the above assumption the conditional probability density of the signal envelope in each of the diversity branch is given by [9]

$$P(w/\gamma) = w \exp(-\frac{w^2 + 2\gamma}{2}) \quad I_0(\sqrt{2\gamma}\, w) \qquad 5-1$$

Where $\gamma$ is the instantaneous power signal to noise ratio

$\quad$ $w$ is the envelope of the output/r.m.s noise $\sqrt{N_0}$

$\quad$ $I_0(\cdot)$ is the Modified Bessel function of the first kind and order zero.

The probability density function of the noise only in each of the diversity branch is given by

$$P(w) = w \exp(-\frac{w^2}{2}) \qquad 5-2$$

However, $\gamma$ is not constant but it is subject to channel conditions. In the next sections the improvement in the FH-MFSK spread spectrum capacity due to the use of space diversity under Rayleigh fading and log-normal shadowing will be evaluated.


## 5-3 Error Probability of Noncoherent On-Off
## Keying with N-Channel Diversity

The conditional probability density function of the square envelope detectors $Y_{in\ell} = w^2$ in each of the diversity branch is given by (using eq. 5-1)

$$P(Y/\gamma) = \tfrac{1}{2} \exp\left(- \frac{Y + 2\gamma}{2}\right) \; I_0(\sqrt{2\gamma Y}) \qquad\qquad 5\text{-}3$$

The probability density function $Y_{in\ell}$ in the case of noise only is given by (using eq. 2)

$$P(Y) = \tfrac{1}{2} \exp\left(- \frac{Y}{2}\right) \qquad\qquad 5\text{-}4$$

a. **Error Probability with Rayleigh Fading only ($\sigma = 0$)**

The p.d.f. of $\gamma$ in eq. 5-3 for Rayleigh fading is given by

$$P(\gamma) = \frac{1}{\gamma_0} \exp\left(- \frac{\gamma}{\gamma_0}\right) \qquad\qquad 5\text{-}5$$

Where $\gamma_0$ is the average signal to noise ratio. Because noise and fading are independent, the p.d.f. of Y can be found by averaging $P(Y/\gamma)$ over $\gamma$, therefore,

$$P(Y) = \begin{cases} \dfrac{1}{2(\gamma_0 + 1)} \exp\left(- \dfrac{Y}{2(\gamma_0 + 1)}\right), & \text{for signal plus noise} \\[4mm] \tfrac{1}{2} \exp\left(- \dfrac{Y}{2}\right) & \text{for noise only} \end{cases} \qquad 5\text{-}6$$

Now, the probability density function of $R_{n\ell} = R$ (the equal gain combining output $R = \sum\limits_{i=1}^{N} Y_{in\ell}$) can be found using characteristic function techniques.

Under the assumption that $Y_i$ are independent, $\phi_R$ the characteristic function of $R_{n\ell}$ is the product of the identical $\phi_Y$ the characteristic function of $Y_i$. Therefore, the p.d.f. of R can be found taking the inverse transform of $\phi_R$ to give

$$P_0(R) = \left(\frac{R}{2}\right)^N \frac{1}{R(N-1)!} \exp\left(- \frac{R}{2}\right) \qquad\qquad 5\text{-}7$$

for noise only, and

$$P_s(R) = \left(\frac{R}{2(\gamma_0 + 1)}\right)^N \frac{1}{R(N-1)!} \exp\left(- \frac{R}{2(\gamma_0 + 1)}\right) \qquad 5\text{-}8$$

with signal present.

The false alarm probability and miss probability can be found using equations 5-7 and 5-8 as the following

$$P_F = P_0[R > \beta^2]$$

$$= \exp\left[-\frac{\beta^2}{2}\right] \sum_{i=0}^{N-1} \frac{(\beta^2/2)^i}{i!} \qquad\qquad 5\text{-}9$$

$$P_D = P_s[R < \beta^2]$$

$$= 1 - \exp\left[-\frac{\beta^2}{2(\gamma_0 + 1)}\right] \sum_{i=0}^{N-1} \frac{[\beta^2/2(\gamma_0 + 1)]^i}{i!} \qquad 5\text{-}10$$

Where $\beta^2$ is the normalized threshold with respect to noise power $N_0$.

b.  **Error probability under the influence of Rayleigh fading and log-normal shadowing**

Unfortunately a closed form expression for $P_D$ similar to equation and 5-10 cannot be found due to the complexity of the p.d.f. of $\gamma$, however, an expression which involves a multiple integral is used in this paper for evaluation the system performance for a realistic values of N up to 3.

The p.d.f. of $\gamma$ under the influence of Rayleigh fading and log-normal shadowing is given by

$$P(\gamma) = \frac{10}{\log_e 10\sqrt{2\pi\sigma^2}} \int_0^\infty \frac{1}{\gamma_0^2} \exp\left(-\frac{\gamma}{\gamma_0}\right) \exp\left[-\frac{1}{2\sigma^2}\left(10\log_{10}\frac{\gamma_0}{\overline{m}_d}\right)^2\right] d\gamma_0$$

$$5\text{-}11$$

Where $\sigma$ is the standard deviation of the log-normal shadowing, typically 6 to 12

$\overline{m}_d$ is the normalized area mean with respect to noise power $N_0$.

The p.d.f. of $Y_{in\ell}$ (signal-present) can be found using eq. 5-3 and 5-11 therefore,

$$P(Y) = \int_0^\infty P(Y/\gamma) \, P(\gamma) \, d\gamma$$

$$= \frac{10/\log_e 10}{\sqrt{2\pi\sigma^2}} \int_0^\infty \frac{1}{2\gamma_0(\gamma_0 + 1)} \exp[- \frac{Y}{2(\gamma_0 + 1)}] \exp[f(\gamma_0)] \, d\gamma_0$$

where $\qquad f(\gamma_0) = - \frac{1}{2\sigma^2} (10 \log_{10} \frac{\gamma_0}{m_d})^2$

5-12

The characteristic function of Y cannot be found in a closed form, hence, the p.d.f. of $R = \sum_{i=1}^N Y_i$ (equal gain combining output) can be found using convolution of $Y_i$, therfore,

$$P_s(R) = \begin{cases} \alpha^2 \int_0^\infty \int_0^\infty \frac{1}{2\gamma_{01} \, \gamma_{02} \, (\gamma_{02} - \gamma_{01})} \left(\exp(- \frac{R}{2(\gamma_{02} + 1)}) - \exp(- \frac{R}{2(\gamma_{01} + 1})\right. \\ \qquad \exp\left[f(\gamma_{01}) + f(\gamma_{02})\right] \, d\gamma_{01} \, d\gamma_{02}, \quad \text{for } N = 2 \\[2em] \alpha^3 \int_0^\infty \int_0^\infty \int_0^\infty \frac{1}{2\gamma_{01} \, \gamma_{02} \, \gamma_{03}(\gamma_{02} - \gamma_{01})} \left\{\frac{\gamma_{02} + 1}{\gamma_{03} - \gamma_{02}} \left(\exp(- \frac{R}{2(\gamma_{03} + 1)})\right.\right. \\ \qquad \left.\exp(- \frac{R}{2(\gamma_{02} + 1)})\right) - \frac{\gamma_{01} + 1}{\gamma_{03} - \gamma_{01}} \left(\exp(- \frac{R}{2(\gamma_{03} + 1)}) - \right. \\ \qquad \left.\left.\exp(- \frac{R}{2(\gamma_{01} + 1)})\right)\right\} \exp[f(\gamma_{01}) + f(\gamma_{02}) + f(\gamma_{03})] \\ \qquad d\gamma_{01} \, d\gamma_{02} \, d\gamma_{03} \qquad \text{for } N = 3 \end{cases}$$

5-13

where
$$\alpha = \frac{10/\log_e 10}{\sqrt{2\pi\sigma^2}}$$

and

$$f(\gamma_{0i}) = -\frac{1}{2\sigma^2} \left(10 \log_{10} \frac{\gamma_{0i}}{\overline{m}_d}\right)^2$$

The assumption is made that $Y_1$, $Y_2$, $Y_3$ are independent and identical random variables which is a reasonable assumption since the antenna separation provides an uncorrelated signal envelope, also shadowing is primarily a function of topography near to the mobile unit, i.e. $\sigma_i = \sigma$ and $\overline{m}_{di} = \overline{m}_d$.

False alarm probability is not a function of signal to noise ratio $\gamma$, therefore, eq. 5-9 can be used for evaluating the system performance for fading and shadowing.

## 5-4  Diversity Improvement in FH-MFSK

The modulation scheme requires a bandwidth of at least $W = \frac{JLD}{K}$ ; that is by assuming that the tones are orthogonal and ignoring the multipath delay spread and doppler shift. Here, we will assume that each user data rate D is 32K bits/sec., and that W = 20 MHz, K = 8 and L = 19.

The modulation capacity curves are shown as broken lines in figures 5-3, 5-4, and 5-5. They are arrived at by following the procedure in [5].

In order to estimate the improvement in the system performance due to space diversity, the receiver operating curves for $\sigma = 0$ are constructed, (solid lines) in figure 5-3, using equations 5-9 and 5-10. Each curve is a contour of $P_F$ and $P_D$ for specified values of the average signal to noise ratio $\gamma_0$ and the number of diversity channel N.

Similarly, the solid lines in figures 5-4 and 5-5 pertain to AWGN with Rayleigh fading and log-normal shadowing $\sigma > 0$.

Now, the system capacity, i.e. the maximum number of simultaneous users the system can accommodate at a certain channel characteristic can be estimated by locating the tangent point of constant M contour and the receiver operating curve on figs. 5-3, 5-4, and 5-5.

Figure 5-3 reveals that the system capacity increased from 30 to 101 users and from 140 to 198 users by using only two diversity branches at $\gamma_0$ = 10 and 20 dB, respectively.

Also, figures 5-4, and 5-5 indicate the large improvement in system capacity by using a moderate number of diversity branches. As an example, the capacity increased from 15 to 70 (the increase is 26.6% relative to the full system capacity 209 users) and from 130 to 195 users by using two diversity branches at $\sigma$ = 12 dB (worst case of shadowing) with $\overline{m}_d$ = 10 and 30 dB, respectively.

Figure 5-6 shows the percent of capacity (relative to the perfect transmission capacity of 209 users) as a function of diversity branch number N with $\gamma_0$ (for $\sigma$ = 0) or $\overline{m}_d$ (for $\sigma$ > 0) as parameters. Also, $\overline{m}_d$ or $\gamma_0$ has been plotted as a function of N with M (number of users) and $\sigma$ as parameters.

## 5-5    Conclusion

Even though Rayleigh fading and log-normal shadowing drastically reduce the system capacity [8], the results obtained here show that the use of diversity can recover much of this capacity loss.

It is clear that the use of diversity permits reliable reception at lower transmitter powers than would be required if space diversity technique was not used. However, this advantage is derived at the cost of added equipment complexity. Figure 5-6 shows the improvement in system capacity for different values of $\sigma$ and $\overline{m}_d$, also, the required signal to noise ratio

$\gamma_0(\sigma = 0)$ or $\overline{m}_d(\sigma > 0)$ has been plotted for constant M and $\sigma$. It is clear that as N increases the required $\gamma_0$ or $\overline{m}_d$ is decreased for constant M and $P_B$, fig. 5-6. As an example, $\overline{m}_d$ will decrease from 40 to 26 dB (for M = 180 users, $\sigma = 12$ dB and $P_B = 10^{-3}$) as N increases from 1 to 2.

The results obtained in this paper reveal that the incremental improvement in the system capacity by adding one more diversity branch decreases as N or $\gamma_0$ (or $\overline{m}_d$) becomes larger, thus indicating that the best value of N (taking into account the system complexity and the amount of improvement) is 2 or 3.

## VI. Adjacent Cell Interference in FH-MFSK Cellular Mobile Radio System

We evaluate quantitatively the effect of adjacent cell interference in cellular mobile system using FH-MFSK transmission. The performance of base to mobile communication in the system, [5], is analyzed, assuming perfect synchronization between users in all the cells. Analysis of the system employing no power control shows that the number of simultaneous users possible at average bit error probability $P_b$ of less than $1 \times 10^{-3}$ is reduced greatly from the corresponding figure for the isolated cell (which is about 170). It is then shown that a simple power control strategy could reduce the adjacent cell interference significantly. A reasonable knowledge of distribution of users within a cell allows the optimization of the receiver threshold with respect to distance from the base. With this optimization, each cell could accomodate $\geq 115$ users at $P_b < 10^{-3}$, the exact figure being dependent on the user-distribution. [16]

### 6-1 Introduction

For the FH-MFSK scheme, it is known that simultaneous number of users that could be handled at a specific bit error rate would decrease when more cells are operating nearby. However, no quantitative assessment has been made so far. Here, we analyze a cellular mobile radio system employing FH-MFSK modulation, with respect to the adjacent cell interference. We assume perfect synchronization between all the users in all the cells and random address assignment for a user in a cell. The power control strategy considered is exclusive to base to mobile transmission and, hence the following analysis is applicable to such a transmission.

Section 6-2 discusses the system in which each cell in a 3-cell cellular system operates with constant power transmission (i.e. no power control). In section 6-3 we analyze the effect of adjacent cell interference in a 3-cell cellular system employing power control. Section 6-4 extends the results of 6-3 to a more general cellular system with six nearest neighbors. This is followed by discussion and conclusion.

## 6-2 Three-Cell Cellular System Without Power Control

Consider a user, u, moving along the line AB in cell of a 3-cell system (fig. 6-1). It is assumed that the propagation delay difference due to the difference in distances kR and $\sqrt{C}$ R (for $0.7 < k < 1$) is small compared to one slot duration $\tau \simeq 13 \mu$ sec. This is true for cells of smaller size. Because of this, orthogonality of received tones is approximately valid.

The user is worst-positioned in the sense that he/she is subject to equal interference from both the nearby cells 2 and 3. Assuming M users are operating in each cell, we calculate below the average probability of bit error, $P_b$ for the user u. We say average probability because the expression arrived at for $P_b$ is by averaging all the probability of bit errors resulting from an ensemble of all possible random address assignment. By looking at figure 1 we can calculate the following.

$SN_1$ = signal to noise ratio at u due to a tone from base 1

$$= 10^{(S - 40 \log k)}$$

Where S is the average SNR in dB when u is in the cell corner.

$SN_2$ = signal to noise ratio at u due to a tone from base 2 or base 3

$$= 10^{(S - 20 \log((1.5-k)^2 + 0.75))}$$

b = Normalized threshold - (normalized with respect to noise at the receiver).

Consider the spurious row of user u. Probability that a tone corresponding to an entry in a spurious row is being transmitted by base 1 or 2 or 3

$$\simeq Pu = 1 - (1 - 2^{-K})^M \qquad\qquad 6\text{-}1$$

where, $K$ = number of bits per transmitted word and $M$ = number of users in any cell.

Define the following:

PF = Probability of false alarm

$$= e^{-b^2/2} \qquad\qquad 6\text{-}2$$

$PE_1$ = Probability of creation of an entry conditioned on the fact that

base 1 transmits the tone corresponding to that entry

$$= \exp(-b^2/2 \ (1 + SN_1)) \qquad\qquad 6\text{-}3$$

$PE_2$ = Probability of creation of an entry conditioned on the fact that

base 2 or 3, but not both, transmits the tone corresponding to that entry

$$= \exp(-b^2/2 \ (1 + SN_2)) \qquad\qquad 6\text{-}4$$

Similarly,

$$PE_3 = \exp(-b^2/2 \ (1 + SN_1 + SN_2)) \qquad\qquad 6\text{-}5$$

$$PE_4 = \exp(-b^2/2 \ (1 + 2 \ SN_2)) \qquad\qquad 6\text{-}6$$

$$PE_5 = \exp(-b^2/2 \ (1 + SN_1 + 2 \ SN_2)) \qquad\qquad 6\text{-}7$$

$$\overline{Pu} = 1 - Pu \qquad\qquad 6\text{-}8$$

Then, the unconditional probability of creation of an entry in the spurious row, which we call the probability of insertion, PI can be calculated as (1) and (2):

$$PI = PF \ \overline{Pu}^3 + Pu \ \overline{Pu}^2 \ PE_1 + 2 \ Pu \ \overline{Pu}^2 \ PE_2 \qquad\qquad 6\text{-}9$$
$$+ 2 \ \overline{Pu} \ Pu^2 \ PE_3 + \overline{Pu} \ Pu^2 \ PE_4 + Pu^3 \ PE_5$$

Next, consider the correct row of user u. Proceeding along similar lines, probability of an entry in the correct row of user u is

$$P_C = Pu^2 \, PE_1 + 2 \, Pu \, \overline{Pu} \, PE_3 + Pu^2 \, PE_5 \qquad \qquad 6\text{-}10$$

Probability of i entries in correct row is

$$P_C(i) = \binom{L}{i} \, P_C^i (1 - P_C)^{L-i} \qquad \qquad 6\text{-}11$$

Using equations (6-9) and (6-11) for PI and $P_C(i)$ respectively and by using the Table 1 of [5] we can calculate $P_b$. With $P_b$ maintained at a value less that $1 \times 10^{-3}$ it is seen that increasing $SN_1$ beyond a certain value does not give a significant return in accomodating more simultaneous users M. Hence, we assume a constant power transmission such that the farthest user in a cell has S = 25 dB at the receiver. Figure 6-2 shows the number of users that could be accomodated at $P_b < 10^{-3}$ for various distances of the worst-positioned receiver from the base i.e. for various kR's, k = 0.7, ... 1. For each k, the threshold b is optimised to minimize $P_b$. It shows that when the worst-positioned receiver is at the cell corner, only 58 users could be accomodated at $P_b < 10^{-3}$ and only 64 users when the worst-positioned receiver is at three-fourth distance from the base to the cell corner. Because of the poor performance of the above system, the need for power control is apparent.

6-3   Three-Cell Cellular System with Power Control

In this section, we calculate the probability of bit error rate $P_b$ for a user u in cell 1 (fig. 6-1), taking into account the effect of adjacent cell interference, assuming each cell operates with power control. Before proceeding to calculate $P_b$ we must consider (a) the power control strategy, (b) propagation delay difference in the arrival of tones from the bases at the user and its effect on synchronization and non-orthogonal interference.

(a) Power Control Strategy:  Consider a set of tones to be transmitted
from base 1, during a slot period.  If more than one user wants to transmit
a particular frequency tone in a time slot, then the control unit at
the base determines the distance of the farthest user requiring the frequency
tone and adjusts the transmitted power, accordingly, so that the farthest
receiver receives a fixed average SNR (say 10 x S dB).

(b) Effect of Propagation Delay Difference:  As in [5], we assume that
non-coherent detection is employed to detect the ON/OFF keyed tones.  The
delay spread [6] in the arrival times of a tone from a base to the user u
is smaller than $\tau$.  Therefore with synchronous transmission from bases, the
received waveforms corresponding to an identical transmitted tone from
bases 1 and 2 would be

$$r_i(t) = a_i \, x \, (t - \tau_{p_i}) \, e^{j \, 2\pi(f_j \, t - \theta_i)} \, , \qquad 0 < t - \tau_{p_i} < \tau \qquad \text{6-12}$$

$$i = 1, 2$$

Here, $\tau_{p_i}$ represents the propagation delay, $a_i$ are independent and Rayleigh
distributed and $\theta_i$ are independent and uniformly distributed.  With power
control it is expected (and verified later) that the interference power from
adjacent cell is small compared to the user interference from the same cell.
Hence, proper synchronization can be assumed in the analysis.  Because of
non-coherent detection, on an average, the effect of ith tone interference
from base 2 at the ith tone detector in u can be calculated assuming inter-
ference over a full slot, (chip), even though in any particular situation,
the interference will be spread over two adjacent slots.

To analyze the non-orthogonal interference from base 2 we consider the reception of $j^{th}$ tone from base 2 in the $i^{th}$ detector of receiver u. The inphase output due to $j^{th}$ tone from base 2 is

$$y_i^j = \int_0^{a\tau} A \sin(\omega_0 + \frac{2\pi}{\tau} i) t \cdot a_2 \sin((\omega_0 + \frac{2\pi}{\tau} j) t + \theta) \, dt \qquad 6-1$$

Let $\quad \tau a_2 \cos \theta \sim$ Normal $(0, \sigma^2)$

$\qquad \tau a_2 \sin \theta \sim$ Normal $(0, \sigma^2)$

then it can be seen that $y_i^j$ conditioned on a $\tau$ is also normally distributed, and

$$\text{variance } [y_i^j / a \, \tau] = \frac{\frac{A^2 \sigma^2}{4}}{\pi^2 (i-j)^2} \sin^2 (\pi (i-j) a) \qquad 6-1$$

It can also be seen that, for $i^{th}$ tone from base 1

$$\text{Var}[y_i^i] = \frac{A^2 \sigma^2}{4} . \qquad 6-1$$

Therefore, only the tones adjacent to the $i^{th}$ tone interfere significantly with the interference power being less than $(\frac{1}{\pi^2 (i-j)^2})$ of that of a possible $i^{th}$ tone. With more than 100 users operating in each cell, probability of $i^{th}$ tone being present at the input to the detector due to users is more than 0.7. Clearly, it is possible to conceive two situations

(i) $i^{th}$ tone present along with other tones

(ii) $i^{th}$ tone not present.

In case (i) neglecting the non-orthogonal interference (17) implies that we are under-estimating the probability of detection slightly and, hence, we have a pessimistic assessment. On the contrary, in situation (ii) the non-orthogonal interference is neglected compared to the noise at the receiver, which can at best be an approximation. With the above observations in mind, we shall neglect the effect of non-orthogonality in the following analysis.

Computation of $P_b$

In order to compute $P_b$, we first compute $SN_0$, the average signal to noise power ratio in the correct row of u due to users in the same cell, IN, the average interference to noise power ratio in the receiver of user u due to users in cell 2 or 3 and $IN_0$, the average interference to noise power ratio in the spurious row of u due to users in the same cell.

(i) Computation of $SN_0$: Consider the time-frequency slot $((i, j), i \in (1...L), j \in (0, 1, \ldots 2^K-1))$ which is detected and transformed as an entry in the correct row of the decoded matrix of user u. Corresponding to this $i^{th}$ slot, $j^{th}$ tone will be transmitted by the base. Because of the power control, the transmitted power in this frequency tone depends on the distance of the farthest user requiring the same tone in the $i^{th}$ slot. It is shown in the Appendix that the probability of more than four users in a cell requiring the transmission of the same tone in the same slot is negligibly small and, hence, we need to consider at most four users in deciding the transmitted power. The calculation of transmitted power is also tied up with the distribution of users within a cell. We assume that the users are distributed uniformly in a cell with respect to distance from the base. If the base station is situated in a highly concentrated downtown area, we could expect the concentration of users to be near the base. However, as will be seen later, the optimum threshold in the receiver depends on the user distribution and, hence, a reasonable knowledge of user distribution within a cell is necessary for best results.

Let $u_n$ be the distance of the farthest user for a n sample user space creating $(i, j)^{th}$ entry in transmitted matrix.

With

$$f_u(u) \sim \text{Uniform } (A1 \times R, \ A2 \times R) \qquad A1 \times R \leq u \leq A2 \times R \qquad \text{6-16}$$

the maximum order statistic $u_n$ has the distribution (after normalizing $u_n$ with respect to cell radius R, i.e. $u_n = R \times \ell_n$,)

$$f_{\ell_n}(\ell) = \frac{n}{(A2 - A1)^n} \ (\ell - A1)^{n-1} \quad A1 \leq \ell \leq A2$$

We shall assume, hereafter, that $A1 = 0.05$ and $A2 = 0.9$. This geometry very closely approximates the hexagonal structure. With the worst-positioned receiver u at distance kR from the base, we have

$$P_n = \text{Probability } [u_n < kR]$$
$$= \text{Probability } [\ell_n < k]$$

Hence

$$P_n = \left(\frac{k - A1}{A2 - A1}\right)^n \qquad \text{6-18}$$

$$\overline{P_n} = 1 - P_n \qquad \text{6-19}$$

Then, the average signal to noise ratio $SN_0$ can be evaluated as follows: Let

$$P_r = 2^{-K}$$

$10 \times S$ = Average SNR in dB at the farthest receiver

M = number of users operating in a cell (assumed same for all cells)

Then,

$$SN_0 = 10^S \ \{(1 - P_r)^{M-1} + \sum_{n=1}^{4} \binom{M-1}{n} P_r^n (1 - P_r)^{M-1-n} \qquad \text{6-20}$$
$$[P_n + \overline{P_n} \ I_{son}/k^4]\}$$

Where

$I_{son} = 4^{th}$ moment (about origin) of $\ell_n$

$$= \int_{A1}^{A2} \ell^4 \ \frac{n}{(A2 - A1)^n} \ (\ell - A1)^{n-1} \ d\ell \qquad \text{6-21}$$

(ii) Computation of IN: It can be noticed that the average interference to noise ratio IN is the same for either the entry in a spurious row or the entry in the correct row of user u. Considering the geometry in figure 1 and defining the distance squared between the base 2 or base 3 to the user u as $CR^2$, we have

$$C = (1.5 - k)^2 + 0.75 \qquad\qquad 6\text{-}22$$

Then, IN can be calculated as follows

$$IN = 10^S \cdot \sum_{n=1}^{4} \binom{M}{n} \, p_r^n \, (1 - p_r)^{M-n} \, I_{In} \qquad\qquad 6\text{-}23$$

Where

$$I_{In} = \frac{1}{C^2} \, I_{son} \qquad\qquad 6\text{-}24$$

(iii) Computation of $IN_0$: Proceeding along the same lines as above, we have

$$IN_0 = 10^S \sum_{n=1}^{4} \binom{M-1}{n} \, p_r^n (1 - p_r)^{M-1-n} \, I_{son}/k^4 \qquad\qquad 6\text{-}25$$

Define the following, as in the previous section.

Probability of false alarm $= PF = e^{-b^2/2}$

$$PE_1 = \exp(-b^2/2(1 + IN_0)) \qquad\qquad 6\text{-}26$$

$$PE_2 = \exp(-b^2/2(1 + IN)) \qquad\qquad 6\text{-}27$$

$$PE_3 = \exp(-b^2/2(1 + IN_0 + IN)) \qquad\qquad 6\text{-}28$$

$$PE_4 = \exp(-b^2/2(1 + 2\ IN)) \qquad\qquad 6\text{-}29$$

$$PE_5 = \exp(-b^2/2(1 + IN_0 + 2\ IN)) \qquad\qquad 6\text{-}30$$

$$Pu_1 = 1 - (1 - 2^{-K})^{M-1} \qquad\qquad 6\text{-}31$$

$$Pu_2 = 1 - (1 - 2^{-K})^{M} \qquad\qquad 6\text{-}32$$

$$\overline{Pu_1} = 1 - Pu_1 \qquad\qquad 6\text{-}33$$

$$\overline{Pu_2} = 1 - Pu_2 \qquad\qquad 6\text{-}34$$

Then PI is given by

$$PI = \overline{Pu_1}\ \overline{Pu_2}^2\ PF + Pu_1\ \overline{Pu_2}^2\ PE_1 + 2\ Pu_2\ \overline{Pu_2}\ \overline{Pu_1}\ PE_2$$

$$+ 2\overline{Pu_2}\ Pu_1\ Pu_2\ PE_3 + \overline{Pu_1}\ Pu_2^2\ PE_4 + Pu_2^2\ Pu_1\ PE_5 \qquad\qquad 6\text{-}35$$

Similarly $P_C$ is given by

$$P_C = \overline{Pu_2}^2\ PE_6 + 2\ Pu_2\ \overline{Pu_2}\ PE_7 + Pu_2^2\ PE_8 \qquad\qquad 6\text{-}36$$

Where

$$PE_6 = \exp(-b^2/2\ (1 + SN_0)) \qquad\qquad 6\text{-}37$$

$$PE_7 = \exp(-b^2/2\ (1 + SN_0 + IN)) \qquad\qquad 6\text{-}38$$

$$PE_8 = \exp(-b^2/2\ (1 + SN_0 + 2\ IN)) \qquad\qquad 6\text{-}39$$

Evaluation and discussion of behavior of $P_b$: With PI and $P_C(i)$ as specified in equations 6-35 and 6-11 and with Table I of [5] we can now calculate $P_b$. Figure 3 shows $P_b$ vs. k for three different values of 10 x S and for few values of M. In each case, the threshold b in the receiver is optimised. That is, the value of b (nearest to 0.5 or 1 or 2 depending on the value of 10 x S of 15 dB or 25 dB or 35 dB) that minimizes $P_b$ is assumed. Following observations are made by looking a figure 6-3.

1.  Increasing 10 x S beyond 25 dB does not give rise to any significant

    reduction in $P_b$.

2.  $P_b$ depends both on the values of k and on M

3.  It is also noticed that $P_b$ peaks for some value near k ≃ 0.5 and falls

off on either side. Therefore, a mobile at the cell corner operates with

much less $P_b$ compared to a mobile near half the distance towards the base.

   With the assumption of power control, the base station knows the radial

distance kR of user u and, hence, by transmitting this information to the mobiles

the threshold can be optimised with respect to the distance. Requiring further

the knowledge of M in each cell at the mobiles seems over-demanding. Hence,

we assume that the optimization of the threshold with respect to distance is

done by assuming that maximum number of users allowed are operating in each cell.

(say 125, as assumed in the sequel). Even though this threshold is suboptimal

when number of users operating in a cell is less than 125, the resulting $P_b$

is less than $2 \times 10^{-3}$ and, hence, such a scheme is acceptable. Accordingly, with

10 x S = 25 dB and b optimised at each k, we get the set of curves $P_b$ vs. M

for various k's as shown in fig.6-4. The result shows that about 118 users can

be operated in each cell in a 3-cell configuration at $P_b \leq 10^{-3}$. Compared to

an isolated channel case, this is a reduction of 30% in spectral efficiency.

6-4  Interference in a General Cellular System

   Figure 6-5 shows the general cellular structure employed in mobile radio.

We consider only the nearest six neighbors in the interference analysis,

since other cells contribute negligibly small interference power. Computation

in the previous section shows that with S=2.5, IN is typically<12dB whereas $IN_0$ an

$SN_0$ are more than 20 dB, thereby implying that the interference from adjacent

cell is small compared to the interference from the same cell. Therefore, we

expect that six adjacent cell configuration should perform nearly as good as

a 3-cell system. Indeed, this is the case as the computations had shown. The principle employed in deriving the equations for the evaluation of $P_b$ is the same as the one in the previous section. Since the equations are many but are not difficult to arrive at, they are not presented here.

Applying the optimization procedure discussed in Section II for fixing the threshold we get fig. 6-6 showing $P_b$ vs. M for various k's. One could observe the closeness of figs. 6-6 and 6-4, supporting our earlier conclusion.

## 6-5 Conclusion

A simple power control scheme has been evaluated to reduce the effect of adjacent cell interference on the performance of FH-MFSK cellular mobile radio system when the users are distributed uniformly within a cell, the results show spectral efficiency reduction of about 32% compared to an isolated cell. Best results can be achieved only with an approximate knowledge of user distribution within a cell. The effect of signal-strength-attenuation with respect to distance on the performance has also been investigated. When the signal strength varies inversely as the cube of distance, about 102 users could be accomodated at $P_b < 10^{-3}$, with the assumed uniform distribution of users within a cell. This results in spectral efficiency reduction of 40% compared to an isolated cell. Certain distribution of users might lead to a better performance than the one arrived at. For example, when the users are distributed Beta(3, 5) with respect to the normalized distance variable k, about 140 users can be accomodated in each cell at $P_b < 10^{-3}$.

We have obtained the above results with the assumption that the non-orthogonal interference due to the differences in the arrival times of tones from different base stations can be neglected. In reality, the non-orthogonal interference is expected to cause some additional degradation in the performance.

## VII. Other Types of Receivers for FH-MFSK Mobile Radio

So far, the analysis has assumed a receiver employing a hard-limited combiner. However, when the receiver detection operation is considered as a hypothesis testing problem, a likelihood receiver would perform the best with the available statistics. In an earlier work [3], Yue analyzed the performance of a likelihood receiver for base to mobile transmission, using some approximate techniques. In a recent paper submitted for publication, we compared the performances of likelihood, linear and hard-limited receivers for base to mobile transmission [18].

In all the receivers, the attempt is to discriminate spurious rows of the decoded matrix of a user, which consists of samples from an exponential-mixture, from the correct row, which consists of samples from a simple exponential density. To assess the performance, we use Chernoff bounding and saddle point integration techniques for evaluating the probability of bit error for likelihood receiver and use an exact method for the linear combiner.

In section 7-1, we briefly discuss various receiver structures for FH-MFSK modulation scheme. In section 7-2 we make an approximate estimate of the likelihood receiver performance. In section 7-2 we also observe the asymptotic equivalence of the likelihood and the hard-limited receivers. The exact probability of error is calculated for a linear combiner in section 7-3.

## 7-1  Receiver Structure for TH-MFSK Modulation

Figure 7-1 shows a section of the non-coherent envelope analyzer. As in [5], let $\tau$ be the chip duration, K be the number of bits of information transmitted every $L\tau$ seconds, W = 20 MHz be the one way bandwidth and R be the bit rate. Then, we have $2^K$ such sections in operation corresponding to different orthogonal tones. Let $\varepsilon_{ij}$ denote the envelope squared output at the $i^{th}$ envelope analyzer after the $j^{th}$ chip. Corresponding to either signal plus noise or noise only case, we have $\varepsilon_{ij}$ to be either exponentially distributed with mean value $(1/\lambda_1)$ or exponentially distributed with mean value $(1/\lambda_0)$, respectively.

A mobile user u receives the signals from the base and creates a decoded matrix every $L\tau$ seconds. The values $\varepsilon_{kj}$ become the entries $X_{ij}$ in the decoded matrix (the decoding is done on the received matrix with the address of user u). In general, a receiver chooses a row as the row corresponding to the transmitted word, based on some decision criterion. In [5], where hard-limited combining is employed, corresponding to each entry (i,j) in the matrix, a number $n_{ij}$ is assigned such that

$$n_{ij} = \begin{cases} 1 & \text{iff} \quad X_{ij} \geq T \\ 0 & \text{otherwise} \end{cases}$$

A row k is declared as the correct row if

$$\sum_{j=1}^{L} n_{kj} \quad > \quad \sum_{j=1}^{L} n_{ij} \qquad\qquad i \neq k$$

-53-

In case two or more rows have the same maximum sum, $\sum$, then any row among these rows is chosen at random as the correct row. In [19], a linear combiner based on choosing the $k^{th}$ row as the correct row such that

$$\max_i \left( \sum_{j=1}^{L} X_{ij} \right) = \sum_{j=1}^{L} X_{kj} \quad \text{was analyzed, for mobile to base transmission,}$$

using some approximate techniques.

Likelihood Receiver: We shall assume that the minimum frequency spacing between the hops in the transmitted waves is larger than the coherent bandwidth of the Rayleigh fading channel. This, then, implies that $X_{ij}$ are independent and exponentially distributed. Among the $2^K$ rows in the decoded matrix, only one row is the correct row, wherein all the $X_{ij}$'s have a mean value $(1/\lambda_1)$. In each of the rest of the $(2^K-1)$ spurious rows, some elements have a mean value of $(1/\lambda_0)$ and the rest have a mean value of $(1/\lambda_1)$. A spurious row has contributions partly from the interfering users plus noise and partly from the receiver noise. On an average, each spurious row will have a proportion, p, of $X_{ij}$'s created due to interference, where p is given by

$$p = 1 - (1 - 2^{-K})^{M-1} \qquad\qquad 7\text{-}1$$

and M equals the number of users operating in the cell.

Since each row can be a spurious row (hypothesis $H_0$) or not (hypothesis $H_1$), we have the following testing problem applied to a $\ell^{th}$ row:

$$H_0: \quad X_{\ell j} \sim p \lambda_1 e^{-\lambda_1 x} + (1-p) \lambda_0 e^{-\lambda_0 x}$$

(vs) 7-2

$$H_1: \quad X_{\ell j} \sim \lambda_1 e^{-\lambda_1 x}$$

where, $\quad j = 1, 2, \ldots L$

$\qquad \ell = 1, \ldots 2^K$

It can be noticed that the proportion, p, is known once the number of users operating in the cell is known. In statistical literature, whereas a lot of attention has been paid to estimate the parameters of a mixture distribution, there has been no significant results concerning the testing of whether a sample originates from a mixture family or from a member of the family and not the mixture.

Normalizing $X_{\ell j}$'s with respect to the received signal, we have

$$Y_{\ell j} = \lambda_1 X_{\ell j} \qquad \qquad 7\text{-}2a$$

Therefore, (2) gets modified as

$$H_0: \quad Y_{\ell j} \sim pe^{-y} + (1-p) be^{-by}$$

vs.

$$H_1: \quad Y_{\ell j} \sim e^{-y} \qquad \qquad 7\text{-}3$$

Where $b = \dfrac{\lambda_0}{\lambda_1}$ , signal plus noise to noise power ratio (SNNR)

Forming the likelihood ratio, we have

$$S_\ell = - \sum_{j=1}^{L} \ell n(p + (1-p) be^{-(b-1)y_{\ell j}}) \qquad \qquad 7\text{-}4$$

Then, the likelihood receiver chooses the row having $\underset{\ell}{Max}\{S_\ell\}$ as the correct row. The block diagram of the likelihood receiver is shown in figure 7-2.

It can be shown that the same receiver can be arrived at by using the approach in [3] with an interference model applicable to base to mobile transmission viz,

$$p(\Gamma_{n\ell}|H_0) = p \, \delta(\Gamma - 1) + (1 - p) \, \delta(\Gamma)$$

$$p(\Gamma_{n\ell}|H_1) = \delta(\Gamma)$$

## 7-2    The Likelihood Receiver Performance

As discussed earlier, we have the decision rule of the likelihood receiver:

Decide the row having the $\underset{\ell}{Max}\{S_\ell\}$ as the correct row.

The statistic $S_\ell$ behaves differently depending on whether $y_{\ell j}$'s belong to $H_0$ or $H_1$ (7-3). However, it is neither possible to find the distribution of $S_\ell$ exactly under either hypothesis, nor possible to calculate exactly the probability of bit error rate.

$$\text{Let} \qquad S_\ell = \sum_{j=1}^{L} Z_{\ell j} \qquad\qquad 7\text{-}5$$

Without loss of generality, let us assume that the $k^{th}$ row is the correct row corresponding to the word transmitted to the user. In other words, all the rows other than the $k^{th}$ row are spurious. Upon finding the distribution of $Z_{\ell j}$ under hypotheses $H_0$ and $H_1$, we have

$$p_{Z_{ij}}(z) = \begin{cases} cd^{-c} \, e^{-2z}(e^{-z}-p)^{c-1} & -\ln(p+d) < z < -\ln p \\ 0 & \text{elsewhere} \end{cases} \qquad 7\text{-}6$$

$$p_{Z_{kj}}(z) = \begin{cases} cd^{-c} \, e^{-z}(e^{-z}-p)^{c-1} & -\ln(p+d) < z < -\ln p \\ 0 & \text{elsewhere} \end{cases} \qquad 7\text{-}7$$

where  $c = 1/(b-1)$

$d = (1-p)b$

$$7\text{-}8$$

## Simple Chernoff bound:

Here we evaluate an upper bound on the probability of bit error using Chernoff method [20]

For identically and independently distributed random variables $X_i$ we have

$$\text{Prob}[\frac{1}{L} \sum_{i=1}^{L} X_i \geq 0] \leq \{E[e^{r_0 x_i}]\}^L \qquad 7\text{-}9$$

Where    $r_0 > 0$ is the Chernoff parameter

We are interested in the probability of bit error $P_b$ given by

$$P_b = \frac{2^{K-1}}{(2^K-1)} \quad (1 - (1 - P_0)^{2^K-1}) \qquad 7\text{-}10$$

Where

$$P_0 = \text{Prob}[S_i - S_k > 0]$$

$$= \text{Prob}[\sum_{j=1}^{L} Z_{ij} - Z_{kj} > 0] \qquad 7\text{-}11$$

Therefore, by upper bounding $P_0$ using (7-9), we can upper bound $P_b$.

Let 
$$y_j = Z_{ij} - Z_{kj} \qquad \text{7-12}$$

Then
$$P_0 = \text{Prob}[\sum_{j=1}^{L} y_j > 0] \le \{E(e^{r_0 y_j})\}^L \qquad \text{7-13}$$

and the parameter $r_0$ is found as the solution to

$$E(y_j e^{r_0 y_j}) = 0 \qquad \text{7-14}$$

The above equation implies that

$$E(Z_{ij} e^{r_0 Z_{ij}}) \, E(e^{-r_0 Z_{kj}}) - E(Z_{kj} e^{-r_0 Z_{kj}}) \, E(e^{r_0 Z_{ij}}) = 0 \qquad \text{7-15}$$

Also,
$$E(e^{r_0 y_j}) = E(e^{r_0 Z_{ij}}) \, E(e^{-r_0 Z_{kj}}) \qquad \text{7-16}$$

Using the density function given in (7-6) and (7-7) it can be shown that

$r_0 = 1/2$ is the only solution to (7-15).

We also observe that

$$E(e^{\frac{1}{2} Z_{ij}}) = E(e^{-\frac{1}{2} Z_{kj}}) \qquad \text{7-17}$$

Therefore, $P_b$ can be upper bounded by numerically evaluating the RHS of
(7-13), using (7-16) and (7-17). Doing this, we arrive at the curves shown as
A in figure 7-4.

Chernoff bound with central limit theorem:

We obtain another approximation to the probability $P_0$ defined in (7-13)
by using the results in [21]. The idea is to derive a tilted density from

the density of $y_j$ (equation (7-12)) and express the probability $P_0$ in terms of the tilted density variable obtained from $y_j$'s. We define

$$p_{T_j}(t) = p_{y_j}(t) \; e^{r_0 t} / E(e^{r_0 y_j}) \qquad\qquad 7\text{-}18$$

and

$$T = \sum_{j=1}^{L} T_j$$

It can be shown that

$$P_0 = [E(e^{r_0 y_j})]^L \int_0^\infty p_T(\alpha) \; e^{-r_0 \alpha} \; d\alpha \qquad\qquad 7\text{-}19$$

and $r_0$ is chosen so as to make $E(T) = 0$. T is the sum of L identically and independently distributed variables and hence, $p_T$ is approximately Gaussian, especially in the vicinity of $E(T) = 0$. The condition $E(T) = 0$ implies that $E(y_j e^{r_0 y_j}) = 0$ and hence, by the results in the previous subsection, $r_0 = \frac{1}{2}$.

We approximate $p_T(\alpha)$ as

$$p_T(\alpha) \approx \frac{1}{\sqrt{2\pi}\; \sigma_T} \; e^{-\alpha^2 / 2\sigma_T^2} \qquad\qquad 7\text{-}20$$

where

$$\sigma_T^2 = L \; \text{var}[T_j]$$

$$= L \left\{ \frac{d^2}{dr_0^2} [E(e^{r_0 y_j})] \Big/ E(e^{r_0 y_j}) \right\}_{r_0 = \frac{1}{2}} \qquad\qquad 7\text{-}21$$

It can be shown that the above bracketed term reduces to

$$\text{Var}(T_j) = 2 \frac{[\int e^{\frac{-3S}{2}}(e^{-S}-p)^{c-1}\,dS][\int S^2 e^{\frac{-3S}{2}}(e^{-S}-p)^{c-1}\,dS]-[\int Se^{\frac{-3S}{2}}(e^{-S}-p)^{c-1}\,dS]^2}{[\int e^{\frac{-3S}{2}}(e^{-S}-p)^{c-1}\,dS]^2}$$

7-22

Where all the integrals are between the limits $(-\ln(p+d),\ -\ln p)$.

Therefore,

$$P_0 \approx (E(e^{r_0 y_j}))^L \int_0^\infty \frac{1}{\sqrt{2\pi}\,\sigma_T} e^{-\alpha^2/2\sigma_T^2} e^{-r_0 \alpha}\, d\alpha, \text{ at } r_0 = \tfrac{1}{2}$$

7-23

Evaluating the RHS of (7-22) numerically, we can evaluate the approximate value of $P_b$ using equations (7-10), (7-16), (7-17) and (7-23). The resulting $P_b$ is plotted against the number of users M in figure 7-4. Comparing this approximate $P_b$ curve against the figure 8 of [5], we see that the likelihood receiver is marginally better than the hard-limited combiner. Though not shown, it was observed that the effect of variation of K on the receiver performance is similar to the one encluntered in the hard-limited combiner, suggesting an optimum K for a given set of W and R. For example, with W = 20 MHz and R = 32 K b/sec., we have the optimum K to be 8.

Asymptotic equivalence of hard-limited and likelihood receivers:

In figure 7-3 we show the plot of the non-linearity

$$F(y) = -\ln(p + (1-p)\, b\, e^{-(b-1)y})$$

7-24

which is nothing but the likelihood ratio. The plot is for fixed p = 0.5 and for various values of b. Several observations can be made by looking

-60-

at the figure. First of all, the function $F(y)$ is non-linear and therefore a receiver based on $\sum y_{ij}$ would not be optimum. Secondly, as $b$ increases, the curve shifts towards the origin, simultaneously making the transition sharper. Ultimately, as $b \to \infty$, the non-linearity becomes degenerate with $F(y) = -\ell n\ p$, $y \neq 0$ and an infinite jump discontinuity at the origin. Therefore, $F(y)$ has a resemblance toward a hard-limiter characteristics, as $b \to \infty$. Moreover, its asymptotic performance is identical to a hard-limiter, as will be shown below.

As $b \to \infty$, the equation 7-3 gets modified as

$$H_0: \quad y_{\ell j} \sim p\ e^{-y} + (1-p)\ \delta(y)$$

$$\text{7-25}$$

$$H_1: \quad y_{\ell j} \sim e^{-y}$$

Therefore, in the correct row, the random variables $Z_{kj} = F(y_{kj})$ are all degenerate taking on values $-\ell n\ p$ with probability one. However, in a spurious row, the random variables $Z_{ij}$ are all identically distributed bernoulli, taking values $-\ell n\ p$ with probability $p$ and $-\infty$ with probability $(1-p)$. Therefore, an error occurs in our decision only when

$$S_k = S_\ell \quad \text{for some } \ell \neq k \qquad\qquad \text{7-26}$$

This can happen only when all the L bernoulli variables take on the value $-\ell n\ p$ and therefore the probability of this event equals $p^L$.

Hence,

$P_1$ = Probability of correctly identifying a row as either spurious or not.

$$\text{7-27}$$

$$= 1 - p^L$$

The above discussion suggests the possibility of more than one row competing for the correct row, though only one exists truly. As in the hard-limited receiver, we resort to random choice of a row among these as the correct row. The probability of correct word decision becomes

$$P_c = \sum_{i=0}^{2^K-1} \binom{2^K-1}{i} P_1^{2^K-1-i}(1-P_1)^i \frac{1}{(i+1)} \qquad 7-28$$

Only the first few terms in the above equation have significant contribution. Finally, the probability of bit error $P_b$ is given by

$$P_b = (1 - P_c) \frac{2^{K-1}}{(2^K-1)} \qquad 7-29$$

The asymptotic bit error rate is plotted as curve D in figure 4.

Now, the hard-limited receiver has a non-linearity of the form

$$F(y) = \begin{cases} 1 & y \geq T \\ 0 & \text{otherwise} \end{cases}$$

Therefore, as $b \to \infty$, equation (7-25) implies that $P_1$ of equation (7-27) also holds good for hard-limited receiver, provided $T \ll 1$. (In reference [5], we need the receiver threshold $\beta \gg 1$, since in this case the normalization of the envelope is done with respect to the receiver noise). Thus, we have established the asymptotic (SNR $\to \infty$) equivalence of likelihood and hard-limited receivers. However, for mobile to base transmission, the saddle point approximation [3] predicts uniformly better performance of the likelihood receiver (approximated as a soft-limiter) over the hard-limited combiner. One reason for this difference could be that the interferers

in mobile to base transmission could contribute energy to some elements of the correct row of the decoded matrix of a user under consideration. Such is not the case with the base to mobile transmission, where the interferers create only the spurious rows.

Saddle point integration:

In the previous subsection on Chernoff bound, we bounded the probability $P_0$, that the sum of L random variables exceeds zero value. Denoting $\phi(u)$ as the characteristic function of the random variable $y_j$ defined in equation (12), we have

$$\Pr\left(\sum_{j=1}^{L} y_j > 0\right) = P_0 = \frac{1}{2\pi i} \int_c \frac{\phi^L(u)}{u} \, du \qquad 7\text{-}30$$

where c is a contour whose real part goes from $-\infty$ to $+\infty$ and whose imaginary part lies in the lower half of the complex u plane. Here, $i=\sqrt{-1}$. The above equation can be rewritten as

$$P_0 = \frac{1}{2\pi i} \int_c \frac{e^{L \ln \phi(u)}}{u} \, du \qquad 7\text{-}31$$

When L is large, the contour c can be deformed into another contour c' such that only a portion of the contour c', around the saddle point, has a dominant contribution to the integral [22]. In fact, it turns out that the first term approximation of the asymptotic expansion of (7-31) is equivalent to the result achieved with Chernoff bound and central-limit theorem.

With $\qquad G(u) = \ln \phi(u) \qquad\qquad 7\text{-}32$

the saddle points are the solutions to

$$G'(u) = \frac{dG(u)}{du} = \frac{\phi'(u)}{\phi(u)} = 0 \qquad\qquad 7\text{-}33$$

Using our results on Chernoff bound, it can be observed that there is a unique saddle point on the imaginary axis at u = -i/2. The deformed contour c' is then the line parallel to the real axis and going through the point -i/2 . On the contour c', Imag[G(u)] is constant and the Re[G(u)] reaches a maximum at -i/2. Therefore, by using the standard saddle point expansion, we can write

$$P_0 \simeq a_0^L \left[ \frac{1}{2\pi i} \int_{-\infty}^{\infty} \frac{e^{-L\left(\frac{a_2}{a_0}\right)\frac{x^2}{2}}}{(x-i/2)} \, dx \right.$$
$$\left. + \frac{1}{2\pi i} \frac{L\,G^{IV}}{24} \int_{-\infty}^{\infty} \frac{e^{-L\left(\frac{a_2}{a_0}\right)\frac{x^2}{2}}}{(x-i/2)} \, x^4 \, dx \right] \qquad 7\text{-}34$$

where
$$a_0 = \phi(u) \Big|_{u = -i/2}$$

$$a_2 = -\frac{d^2\phi(u)}{du^2} \Big|_{u = -i/2}$$

$$G^{IV} = \frac{d^4 G(u)}{du^4} \Big|_{u = -i/2}$$

In figure 7-4 we show as curve c, the probability of bit error $P_b$ of equation 7-10, when $P_0$ is computed using 7-34. We notice that the inclusion of the second term as in the RHS of (7-34) resulted only in very little change in $P_b$ (observe the closeness of curves B and C). Also, the curve c at 35 dB SNNR lies slightly below the theoretical infinite SNNR curve D. This discrepancy

can be attributed only to the saddle point approximation technique. Since L is not really large (L = 19), the interaction between the pole at the origin of the integrand in (7-31) and the not too far saddle point at -1/2 must be considered. Therefore, more refined saddle point technique is needed for a better estimate. Assuming that the optimism of curve c at 35 dB SNNR is retained at 25 dB SNNR, and with $P_b < 10^{-3}$ we observe that only about 15 users more than that is possible with a hard-limited receiver could be accomodated (See figure 7-4; also recall that the hard-limited receiver can accomodate about 170 users under the same conditions). This suggests that the likelihood receiver is only marginally superior to a hard-limited receiver.

## 7-3    Linear Combining Receiver:

Based on our exponential mixture model, we can evaluate the probability of bit error for the linear combiner, without invoking any approximations.

Let

$$S_\ell = \sum_{j=1}^{L} y_{\ell j} \qquad\qquad 7\text{-}35$$

where $y_{\ell j}$ are distributed as in equation (7-3). The receiver chooses the row m as the correct row such that $S_m = \underset{\ell}{\text{Max}}(S_\ell)$. It is of interest to find the distribution of $S_\ell$ under $H_0$ and $H_1$. As before, assume that $k^{th}$ row is the correct row and all $i \neq k$ are spurious. Then

$$S_k \sim \text{Gamma } (L, 1)$$

i.e.

$$P_{S_k}(S) = \begin{cases} \dfrac{S^{L-1}}{\Gamma(L)} \; e^{-S} & S \geq 0 \\ \\ 0 & \text{Otherwise} \end{cases} \qquad\qquad 7\text{-}36$$

We find the distribution of $S_i$ through the use of characteristic functions. Precisely,

$$P_{S_i}(S) = \frac{1}{2\pi} \int_{-\infty}^{\infty} \left[ \left(\frac{p}{1-it}\right) + \frac{(1-p)b}{b-it} \right]^L e^{-itS} \, dt \qquad 7\text{-}37$$

The above equation can be rewritten as

$$P_{S_i}(S) = \sum_{m=0}^{L} \binom{L}{m} p^m ((1-p)b)^{L-m} \left[\frac{1}{2\pi} \int_{-\infty}^{\infty} \frac{e^{-itS} \, dt}{(1-it)^m (b-it)^{L-m}} \right] \qquad 7\text{-}38$$

Evaluating the integral in the above equation using the residue theorem we have

$$P_{S_i}(S) = \left[ \frac{[(1-p)b]^L (-1)^{L-1}}{(L-1)!} \, S^{L-1} \, e^{-bS} \right.$$

$$+ \sum_{m=1}^{L-1} \binom{L}{m} p^m ((1-p)b)^{L-m} \left\{ \frac{(-1)^{m-1}}{(m-1)!} \sum_{k=0}^{m-1} \binom{m-1}{k} \right.$$

$$[(L-m)\ldots(L-m+k-1)] \, (1-b)^{-L+m-k} \, S^{m-k-1} \, e^{-s}$$

$$+ \frac{(-1)^{L-m-1}}{(L-m-1)!} \sum_{k=0}^{L-m-1} \binom{L-m-1}{k} [m(m+1)\ldots(m+k-1)] \, (b-1)^{-m-k}$$

$$\left. S^{L-m-1-k} \, e^{-bs} \right\} + \left. \frac{p^L (-1)^{L-1}}{(L-1)!} \, S^{L-1} \, e^{-S} \right] (-1)^{L+1} \qquad S \geq 0 \qquad 7\text{-}39$$

$$= 0 \qquad \text{otherwise}$$

Above, the terms $[(L-m)\ldots(L-m+k-1)]$ and $[m(m+1)\ldots(m+k-1)]$ equal 1 when $k=0$. Therefore, the probability of bit error $P_b$ can be calculated as

$$P_b = \frac{2^{K-1}}{2^K - 1} \; (1 - P_1^{2^K - 1}) \qquad\qquad 7\text{-}40$$

where

$$P_1 = \text{Prob}[S_k > S_i]$$

$$= \int_0^\infty F_{S_i}(s) \; p_{S_k}(s) \qquad ds \qquad\qquad 7\text{-}41$$

and $F_{S_i}(s)$ is the distribution function of the density function given in 7-39. $P_b$ was evaluated numerically using a computer and the results are shown in figure 7-5. It is seen that the linear combiner performs very poorly. Similar dismal performance of the linear combiner with respect to mobile to base transmission was established in [19].

## 7-4  Conclusion

Considering the base to mobile transmission, we compared the performance of the likelihood, hard-limited and linear combining receivers. The linear combiner performs the worst, agreeing with the expectations, after observing the performance in the mobile to base link. A simple Chernoff bound technique gives an upper bound on the probability of bit error for the likelihood receiver. The bound is not very tight, but assures a minimum performance. As SNR $\to \infty$, it is shown that the theoretical considerations imply the equivalence of hard-limited and likelihood receivers. This is slightly different from the mobile to base link, where the likelihood receiver seems to have a slightly better performance than the hard-limited receiver [3].

We observed, by employing saddle point integration, that the likelihood receiver is only marginally superior to a hard-limited receiver at finite SNNR and hence, because of the simplicity of implementation, the latter is to be preferred. Also, it is noticed that a refined saddle point integration technique is required for a better error estimate.

REFERENCES

1.  G.R. Cooper, R.W. Nettleton, "A Spread-Spectrum Technique for High Capacity Mobile Communications", IEEE Trans. on Veh. Tech., Vol. VT-27, No. 4, November, 1979.

2.  R.W. Lucky, J. Salz and E.J. Weldon, Jr., "Principles of Data Communications", New York, McGraw-Hill, 1968, pp. 255.

3.  O.C. Yue, "Maximum Likelihood Combining for Non-Coherent and Differentially Coherent Frequency-Hopping Multiple-Access Systems", IEEE Transactions, IT, Vol. IT-28, No. 4, July, 1982, pp. 631-639.

4.  P.S. Henry, "Spectrum Efficiency of a Frequency-Hopped DPSK Spread Spectrum Mobile Radio System", IEEE Trans. on Veh. Tech., Vol. VT-28, No. 4, November, 1979.

5.  D.J. Goodman, et. al., "Frequency-Hopped Multilevel FSK for Mobile Radio", BSTJ, Vol. 59, No. 7, September, 1980, pp. 1257-1275.

6.  W.C. Jakes, "Microwave Mobile Communication", John Wiley and Sons, New York, 1974.

7.  R.H. Muammar and S.C. Gupta, "Performance of a Frequency Hopped MFSK Spread Spectrum Mobile Radio System", IEEE Transactions on Veh. Tech., Vol. VT-31, No. 2, May, 1982.

8.  R. Muammar and S.C. Gupta, "Performance of a Frequency Hopped Multilevel FSK Spread Spectrum Receiver in a Rayleigh Fading and Lognormal Shadowing Channel", International Communications Conference, ICC '82, Conference Record, Vol. 3, pp. 6B.6.5.

9.  M. Schwartz, W.R. Bennett and S. Stein, "Communication Systems and Techniques", New York, McGraw-Hill, 1966.

10. Richard C. French, "The Effect of Fading and Shadowing on Channel Reuse in Mobile Radio", IEEE Trans. Veh. Tech., Vol. VT-28, No. 3 August, 1979, pp. 171-181.

11. G.A. Arredendo, J.I. Smith, "Voice and Data Transmission in Mobile Radio Channel at 850 MHz", IEEE Transactions Veh. Tech., Vol., VT-26, No. 1, February, 1977, pp. 88-93.

12. G.A. Arredendo, J.C. Feggeler and J.I. Smith, "Voice and Data Transmission", BSTJ, Vol. 58, No. 1, Jan. 1979, pp. 97-123.

13. W.C. Jakes Jr., "A Comparison of Specific Space Diversity Techniques for Reduction of Fast-Fading in UHF Mobile Radio Systems", IEEE Trans. on Veh. Tech., Vol. VT-20, No. 6, November, 1971.

14. O.C. Yue, "Useful Bounds on the Performance of a Spread Spectrum Mobile Communication System in Various Fading Environments", IEEE Trans. on Comm., Vol. COM-28, No. 10, Oct., 1980, pp. 1819-1823.

15. R. Muammar and S.C. Gupta, "Diversity Improvement in Frequency Hopping Multilevel FSK Systems under the influence of Rayleigh Fading and Log-normal Shadowing", paper #A.3.7, Globecom '82, Vol. 1, Conference Record. Also to appear in IEEE Trans. on Comm.

16. R. Viswanathan and S.C. Gupta, "Adjacent Cell Interference in FH-MFSK Cellular Mobile Radio Systems", paper #A.3.4, Globecom '82, Vol. 1, Conference Record.

17. R. Viswanathan and S.C. Gupta, "Burst Error Analysis of Frequency-Hopping Systems for Mobile Communication", International Communication Conference, ICC '82, Conference Record, Vol. 3, pp. 5B.4.1 - 5B.4.4.

18. R. Viswanathan, S.C. Gupta, "Performance Comparison of Hard-Limited Likelihood and Linear Combining Receivers for FH-MFSK Mobile Radio", Submitted for IEEE Trans. on Communications.

19. O.C. Yue, "Performance of Frequency-Hopping Multiple Access Multilevel. FSK Systems with Hard-Limited and Linear Combining", IEEE Transactions on Comm. Vol. COM-29, No. 11, Nov. 1981, pp. 1687-1694.

20. J.M. Wozencraft, I.M. Jacobs, _Principles of Communication Engineering_, John Wiley and Sons, N.Y., 1966, pp. 97-102.

21. I.M. Jacobs, "Probability-of-Error Bounds for Binary Transmission on the Slowly Fading Rician Channel", IEEE Trans. IT, vol. IT-12, No. 4, October, 1966, pp. 431-441.

22. A. Erdelyi, _Asymptotic Expansions_, Dover Publications, 1956.

Message
data
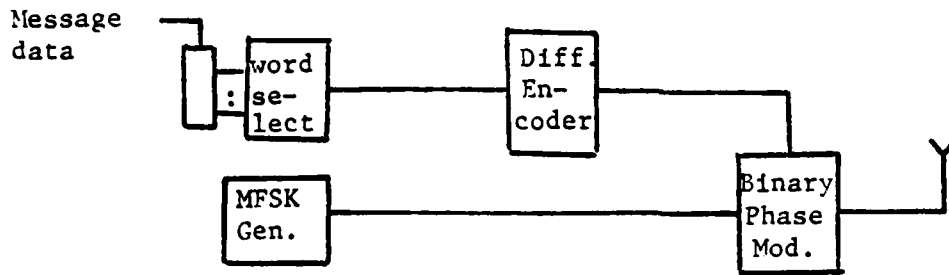


Figure 1-1    Transmitter in FH-DPSK system
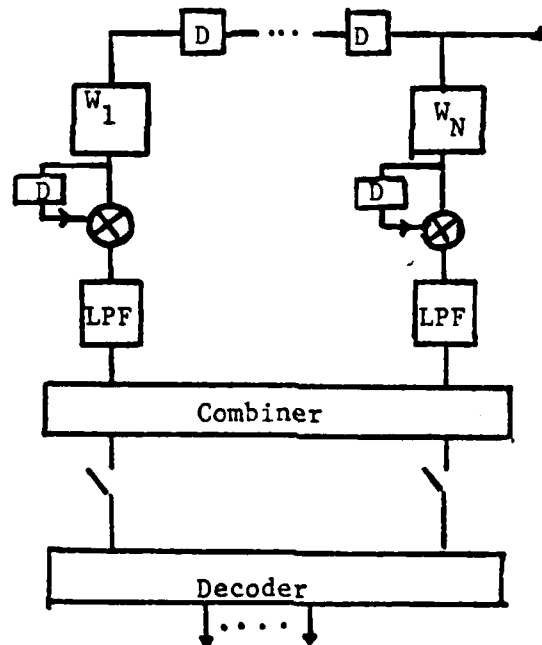


Figure 1-2    Receiver in FH-DPSK system

Binary input
$R_b$ bits/sec.

```
         ┌────────┐          Mod $2^K$        ┌──────────┐
─────────│ Buffer │────────────( + )──────────│ Tone gen │──────── Transmitted
         └────────┘             │             └──────────┘          Signal
                                │
                           ┌─────────┐
                           │ Address │
                           └─────────┘
```
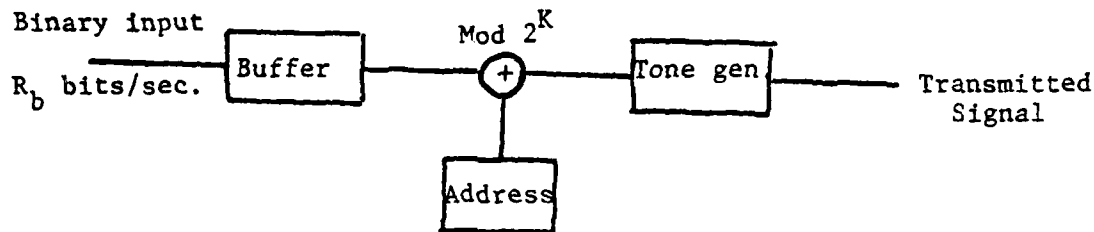
Figure 1-3  Transmitter in FH-MFSK


Received                        Mod $2^K$
Signal

```
         ┌──────────┐          +              ┌───────────┐
─────────│ Spectrum │──────────( )────────────│ Code Word │─────────
         │ Analyzer │          −              │  Decoder  │
         └──────────┘          │              └───────────┘
                               │
                          ┌─────────┐
                          │ Address │
                          └─────────┘
```
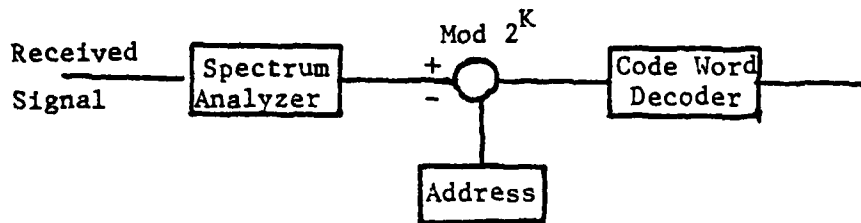
Figure 1-4    Receiver in FH-MFSK
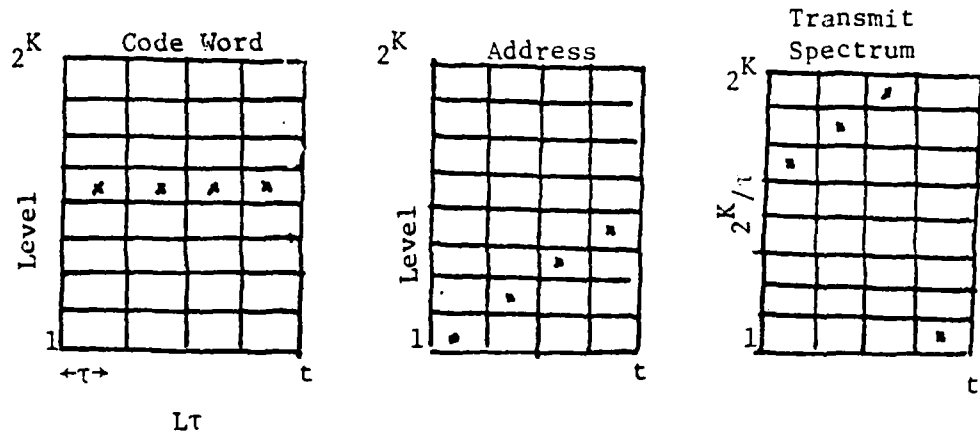
Figure 1-5a    Matrices in Transmit Portion
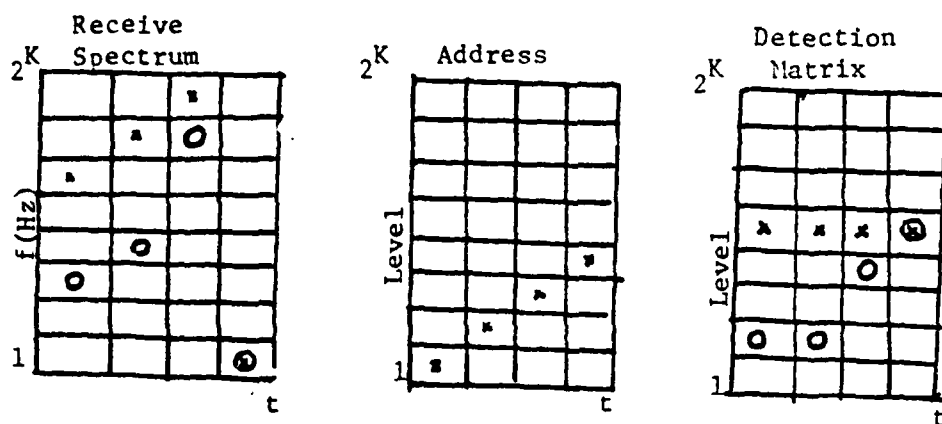


Figure 1-5b    Matrices in Receive portion.  The matrices
show reception of the frequencies in Figure 11a (X)
and reception of a set of tones (0) transmitted
by one other user.
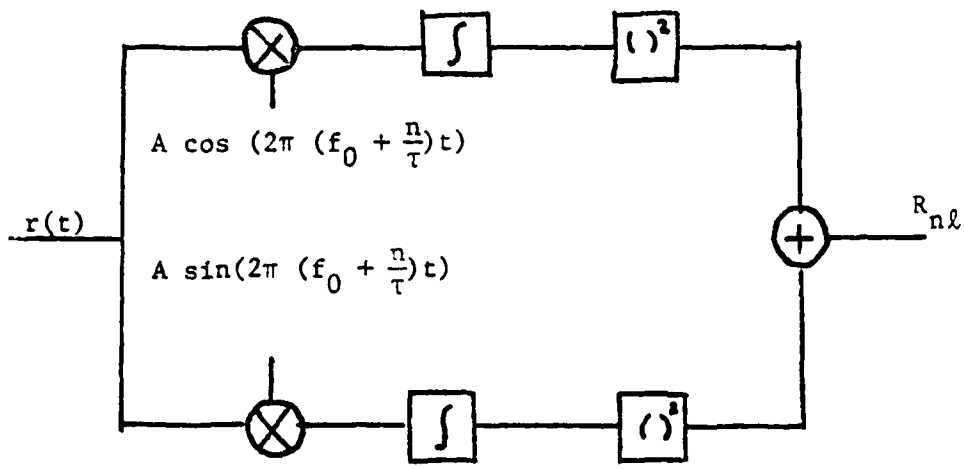
Figure 1-6  Envelope analyzer for $n^{th}$ frequency

$R_{n\ell}$ - output in $\ell^{th}$ chip
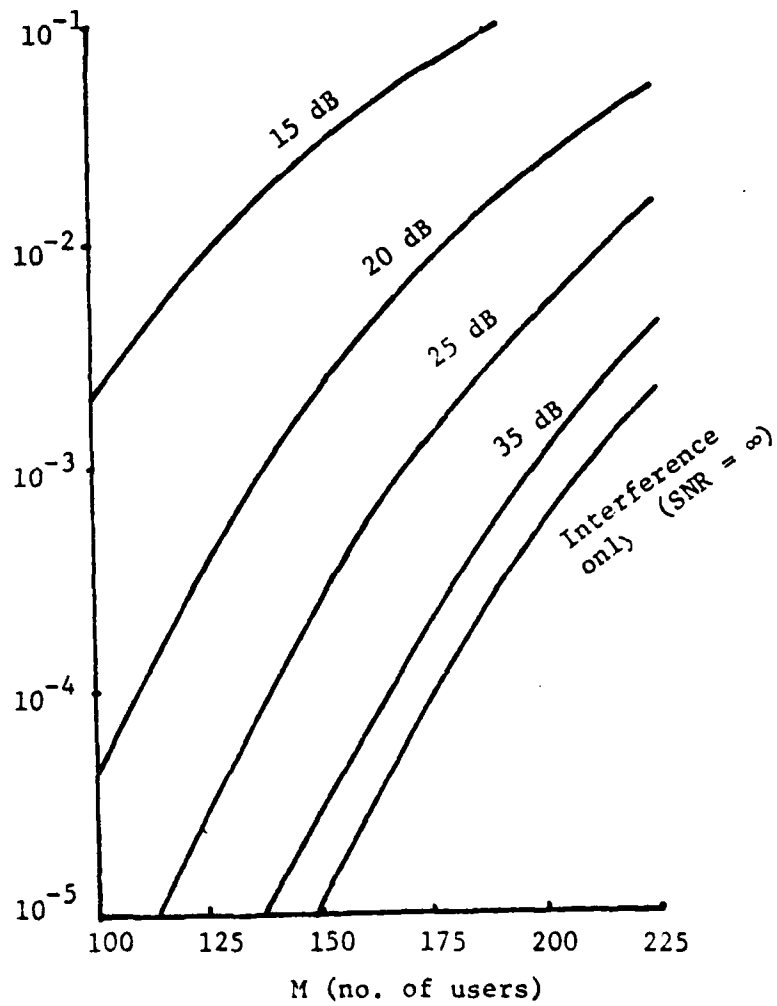


Figure 1-7   Hard-limited receiver performance
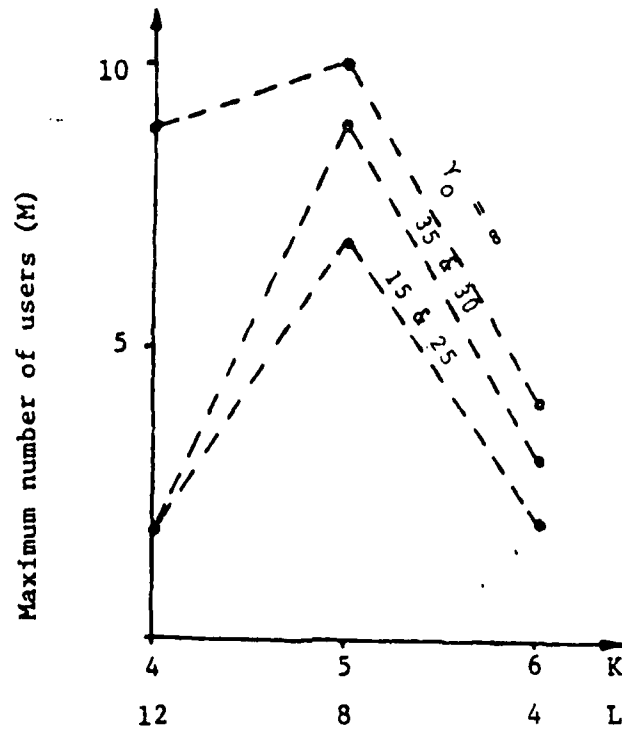
Fig. 2-1 Maximum number of users vs. K message block size, for W = 1.64 MHz.
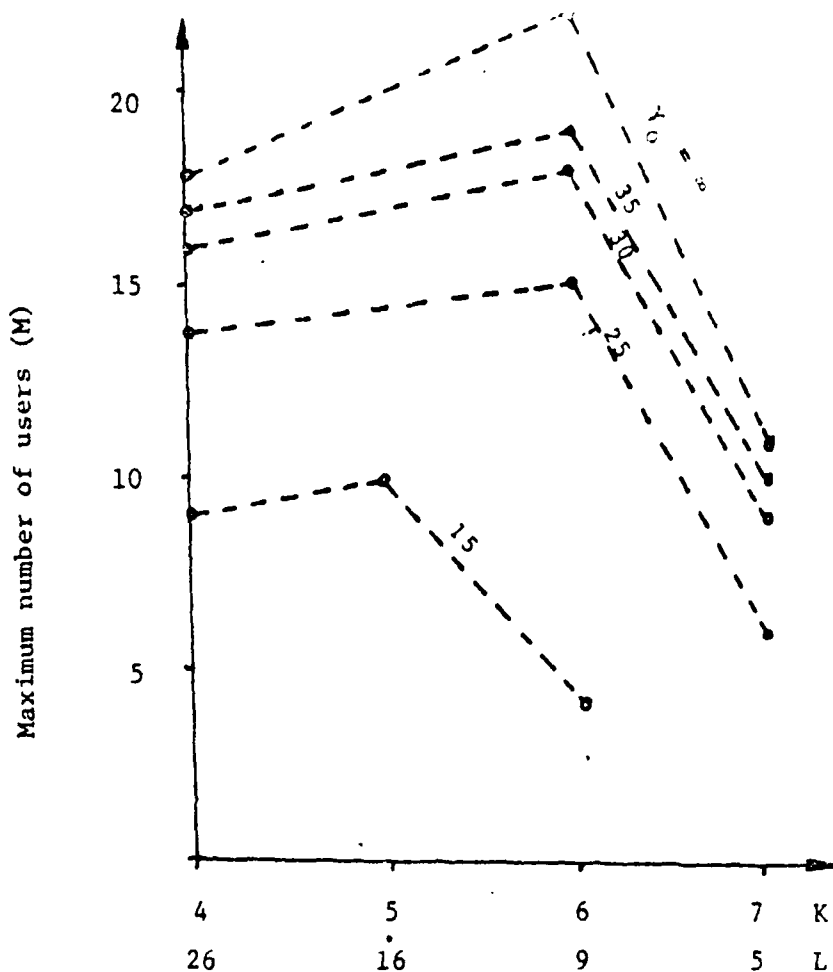
Fig. 2-2 Maximum number of users vs. K message block size, for W = 3.41 MHz.
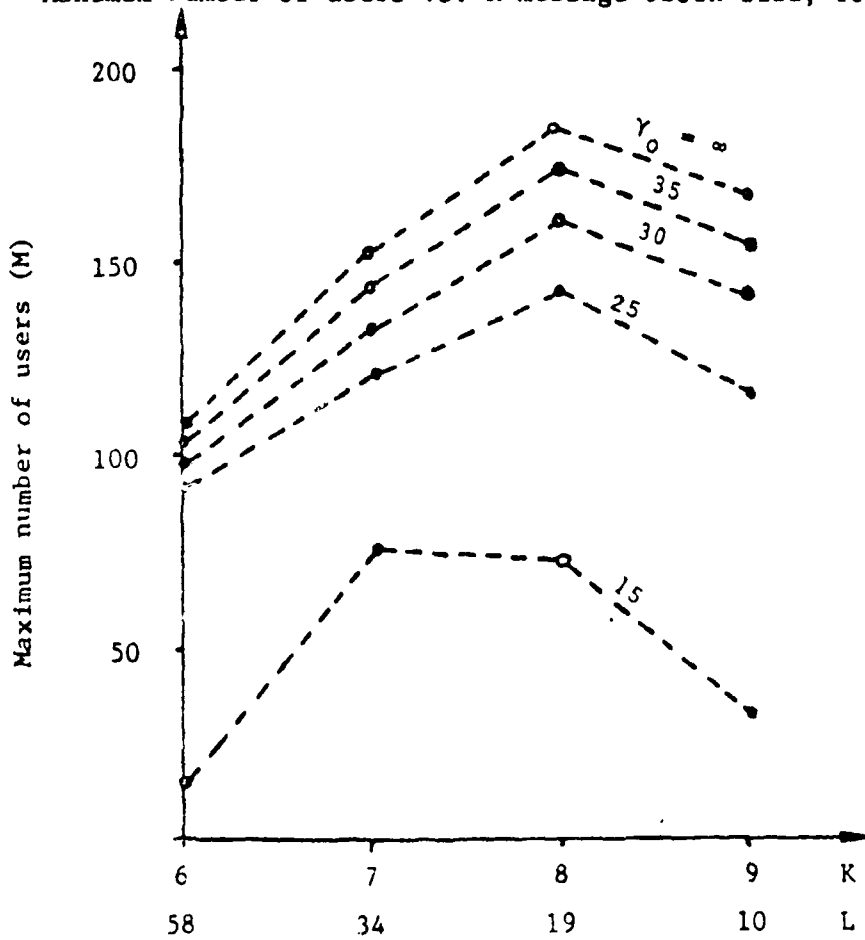


Maximum number of users vs. K message block size for W = 20 MHz.
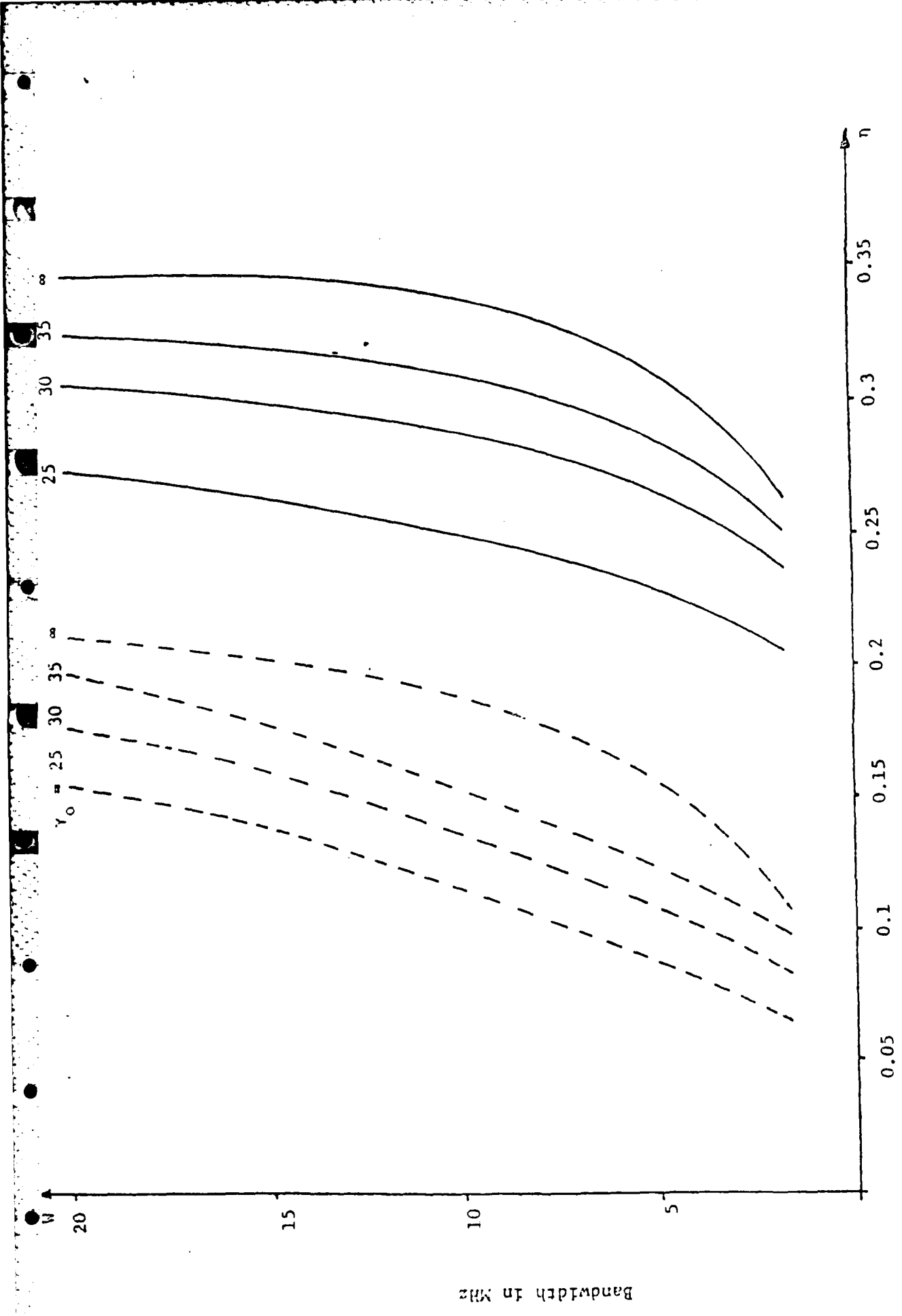
Fig. 2-4 Bandwidth vs. spectrum efficiency for $P_B = 10^{-3}$ (solid), $P_B = 10^{-6}$ (broken).
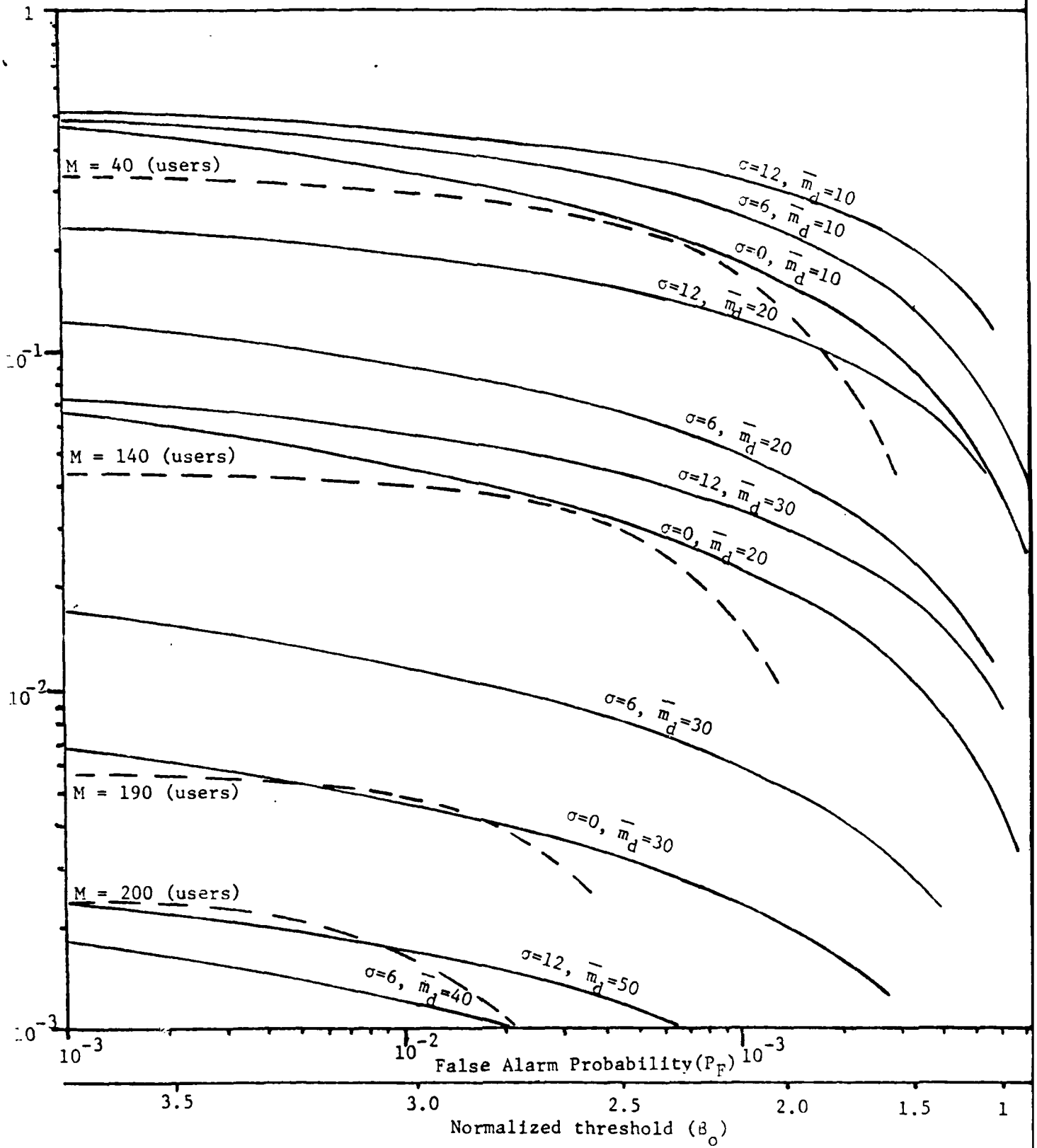
Fig. 3-1 Constant M contour (broken), and receiver operation curve solid for $\sigma=0$, 6 and 12 dB, K=8, L=19, at bit error probability $P_B=10^{-3}$.
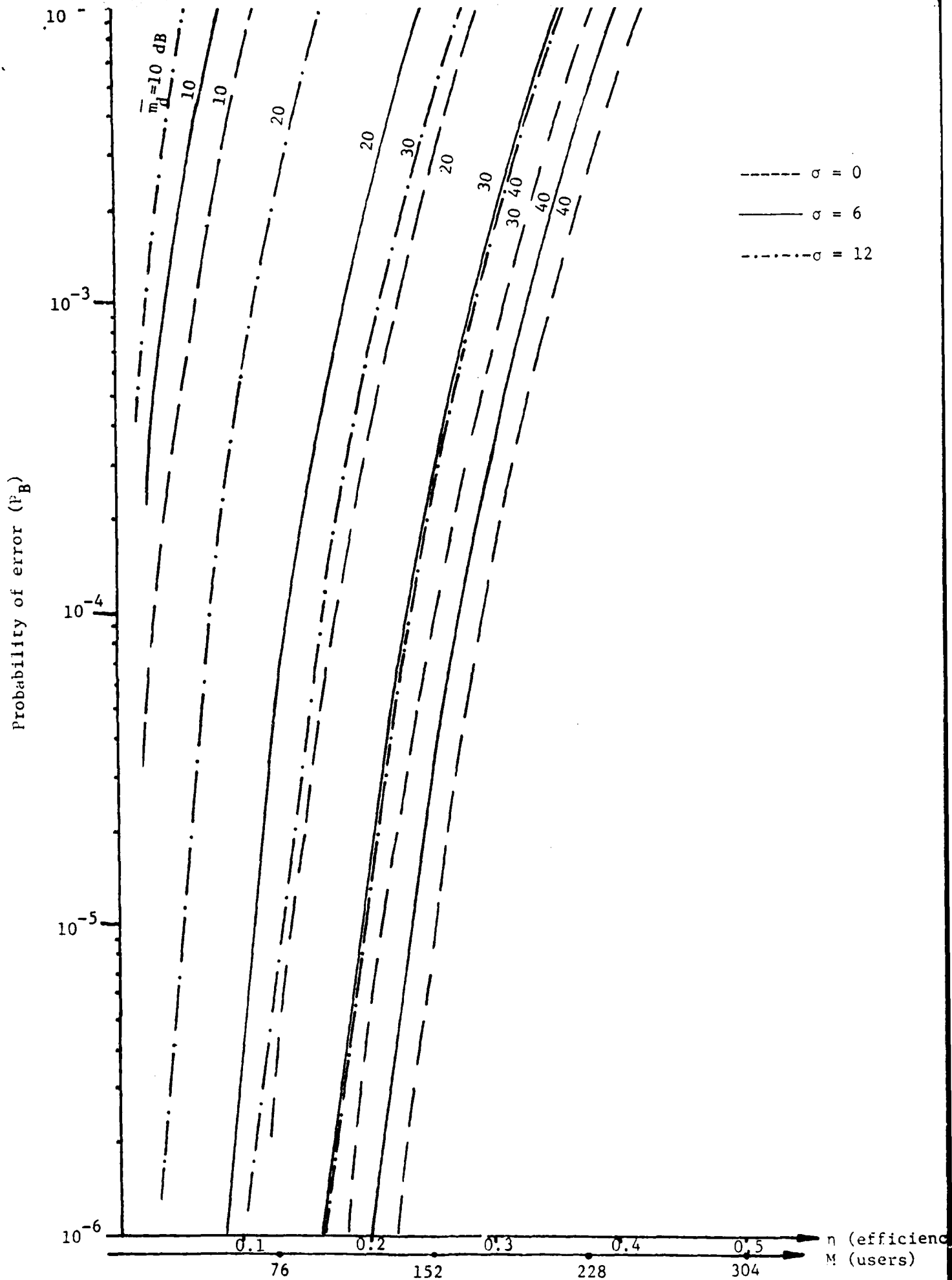
Fig. 3-2 Average probability of error vs. efficiency for $\sigma=0$, 6 and 12 dB, W=20 MH
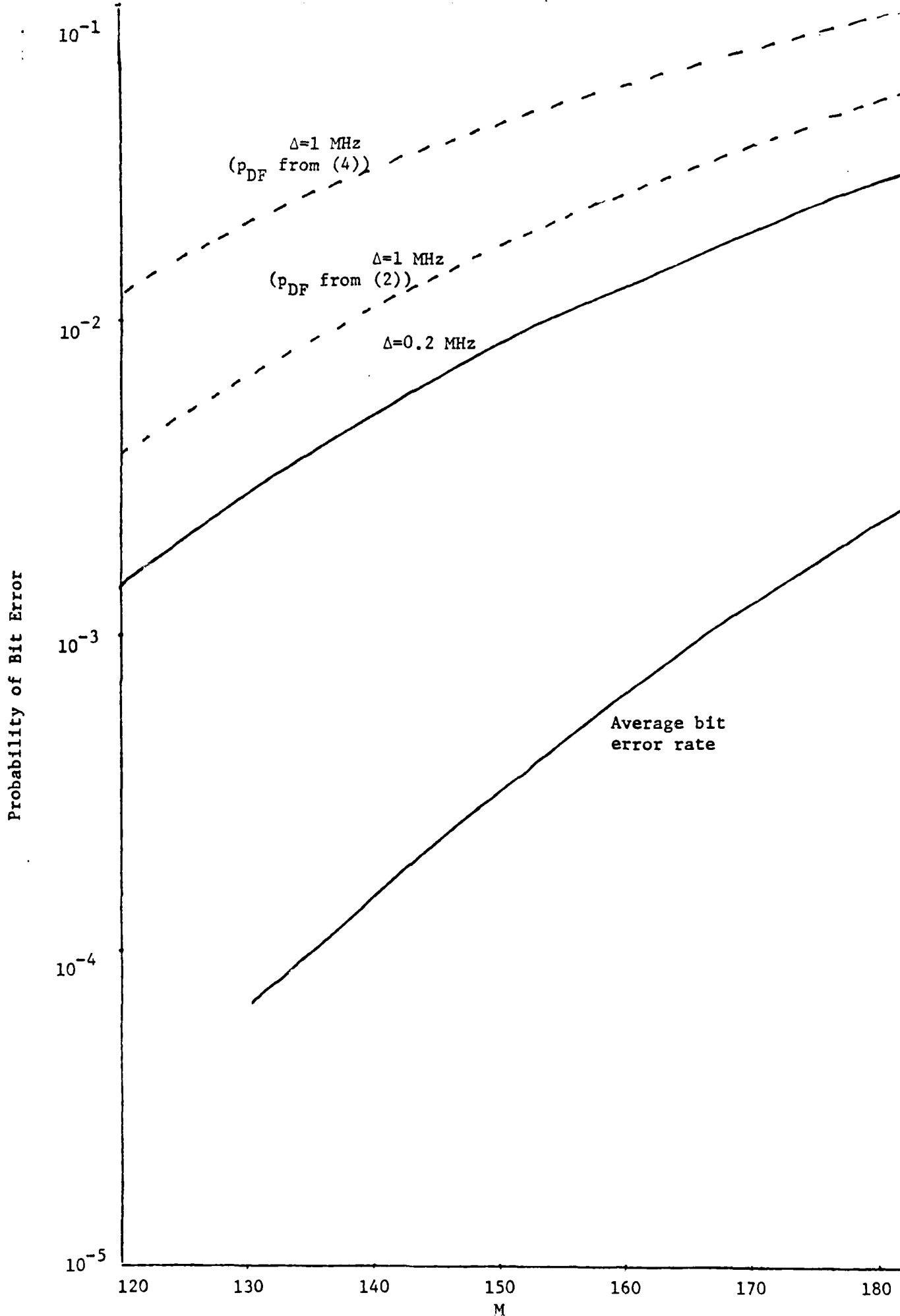
Fig. 4-1  Probability of bit error vs. No. of users for FH-FSK
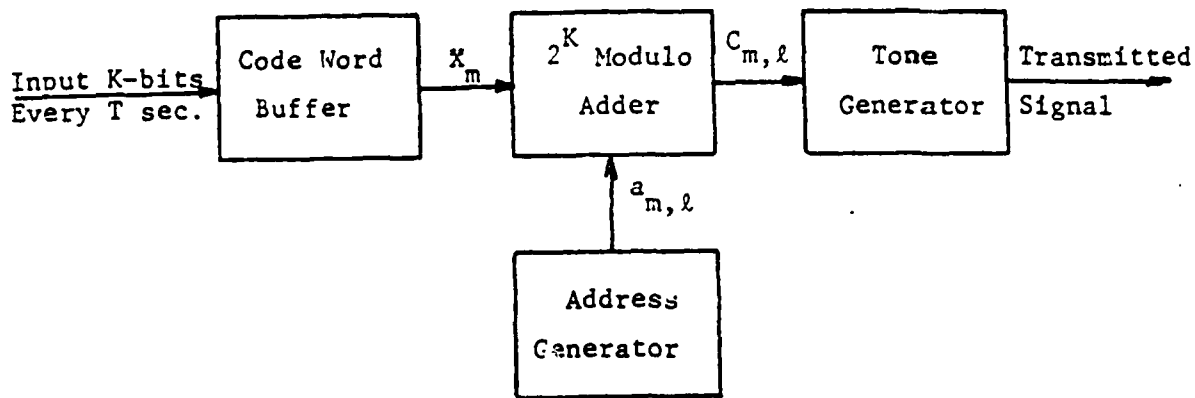
Figure 5-1 Simplified Block diagram of FH-MFSK Transmitter



$$\hat{R}_{i\ell} = \begin{cases} 1 & \text{if } R_{i\ell} > \beta^2 \\ 0 & \text{otherwise} \end{cases}$$

$k^{th}$ receiver with J-energy detector
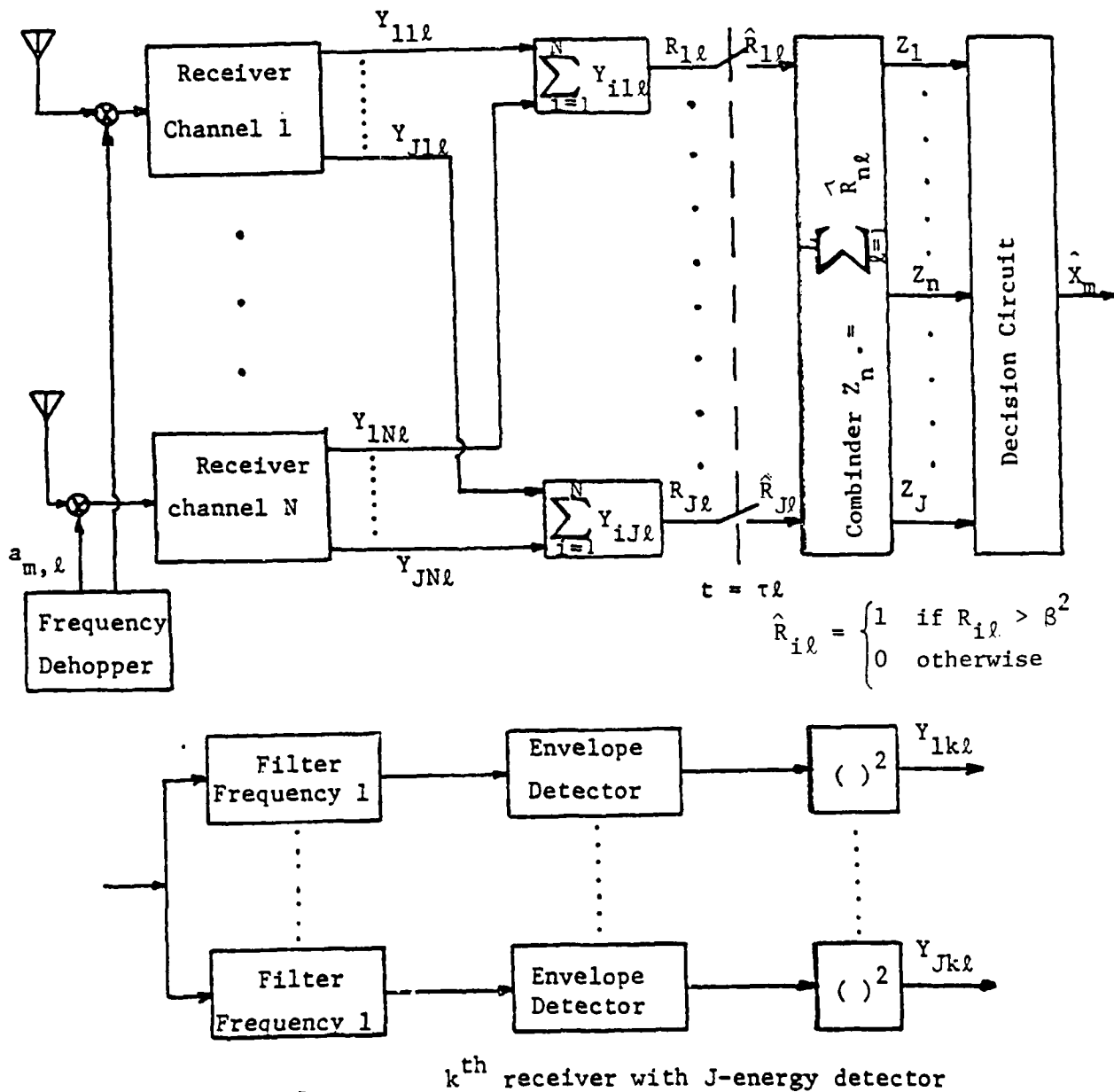
Fig. 5-2  FH-MFSK Receiver with N diversity channel.  The decision circuit

chooses $\hat{X}_m$ corresponding to $Z_m = \max \{Z_1, \dots Z_J\}$

-)-
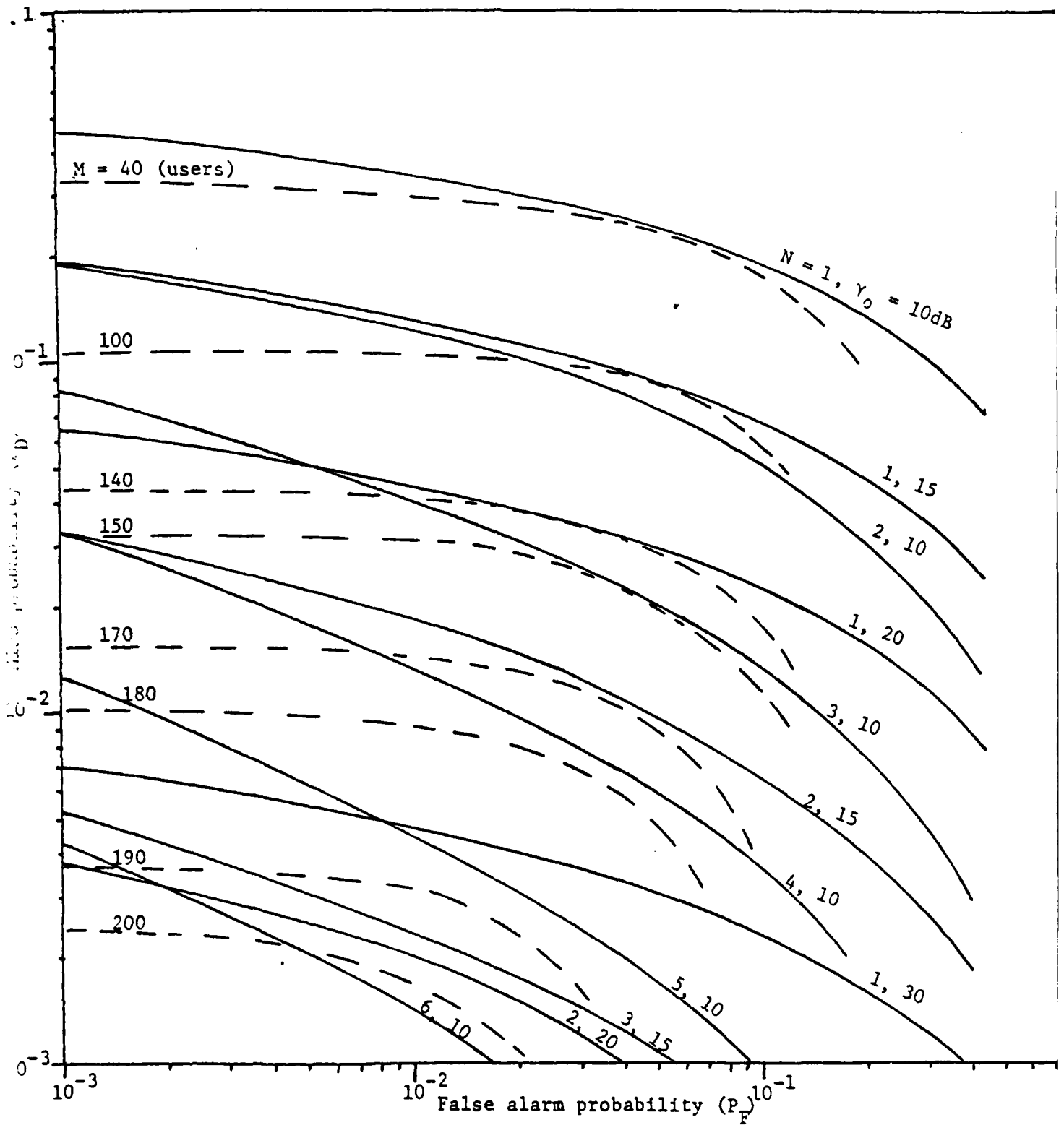
Figure 5-3 Constant M contour (broken) at an average bit error probability $P_B = 10^{-3}$ with $\hat{K} = 8$ and $\hat{L} = 19$. The receiver operation curve (solid) for $\sigma = 0$ (fading only) with N and $\gamma_o$ as parameters.
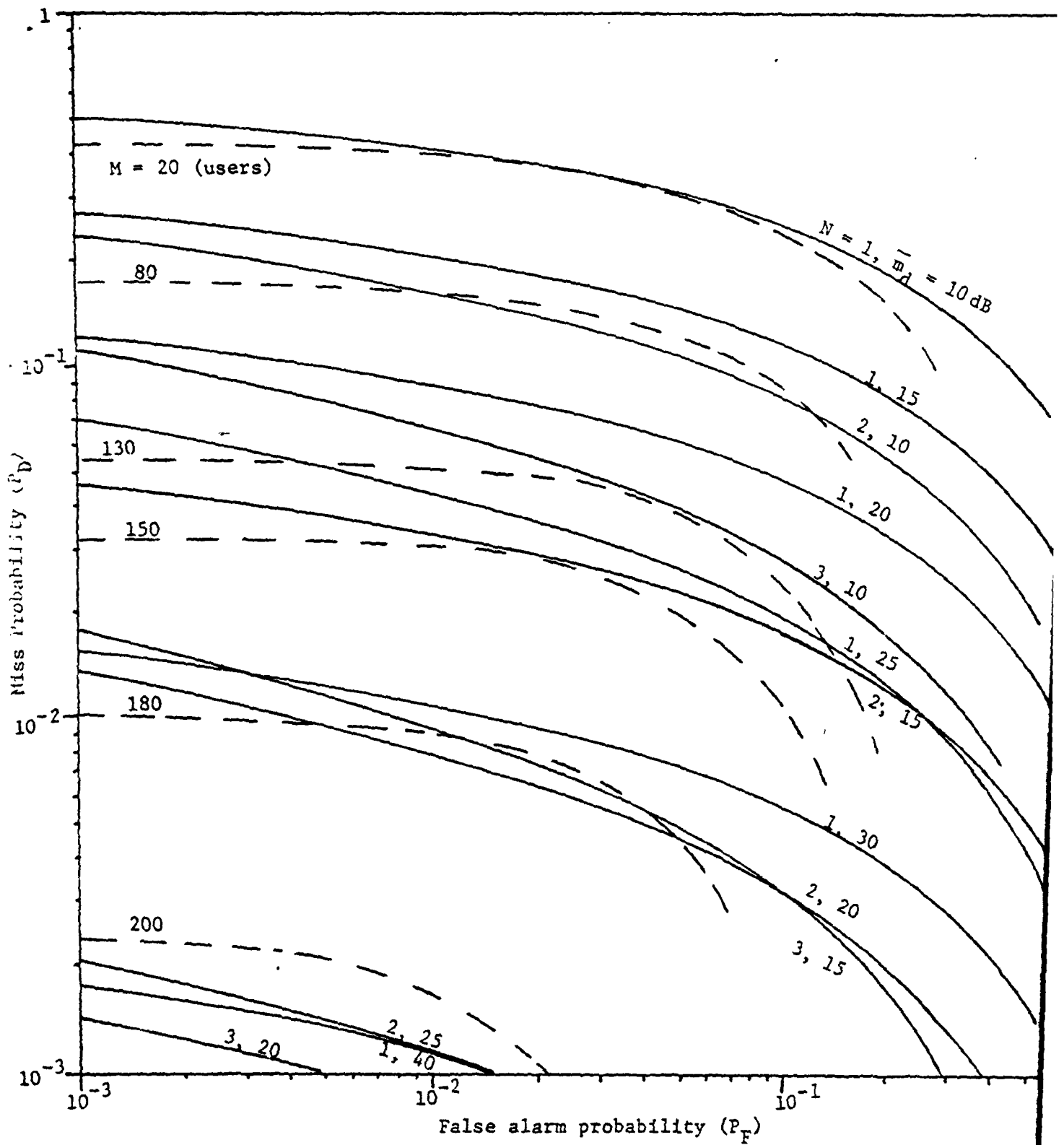
Figure 5-4 Constant M contour (broken) at an average bit error probability $P_B = 10$
with $\hat{K} = 8$ and $\hat{L} = 19$. The receiver operation curve (solid) for $\sigma = 6$
with N and $\overline{m}_d$ as parameters.
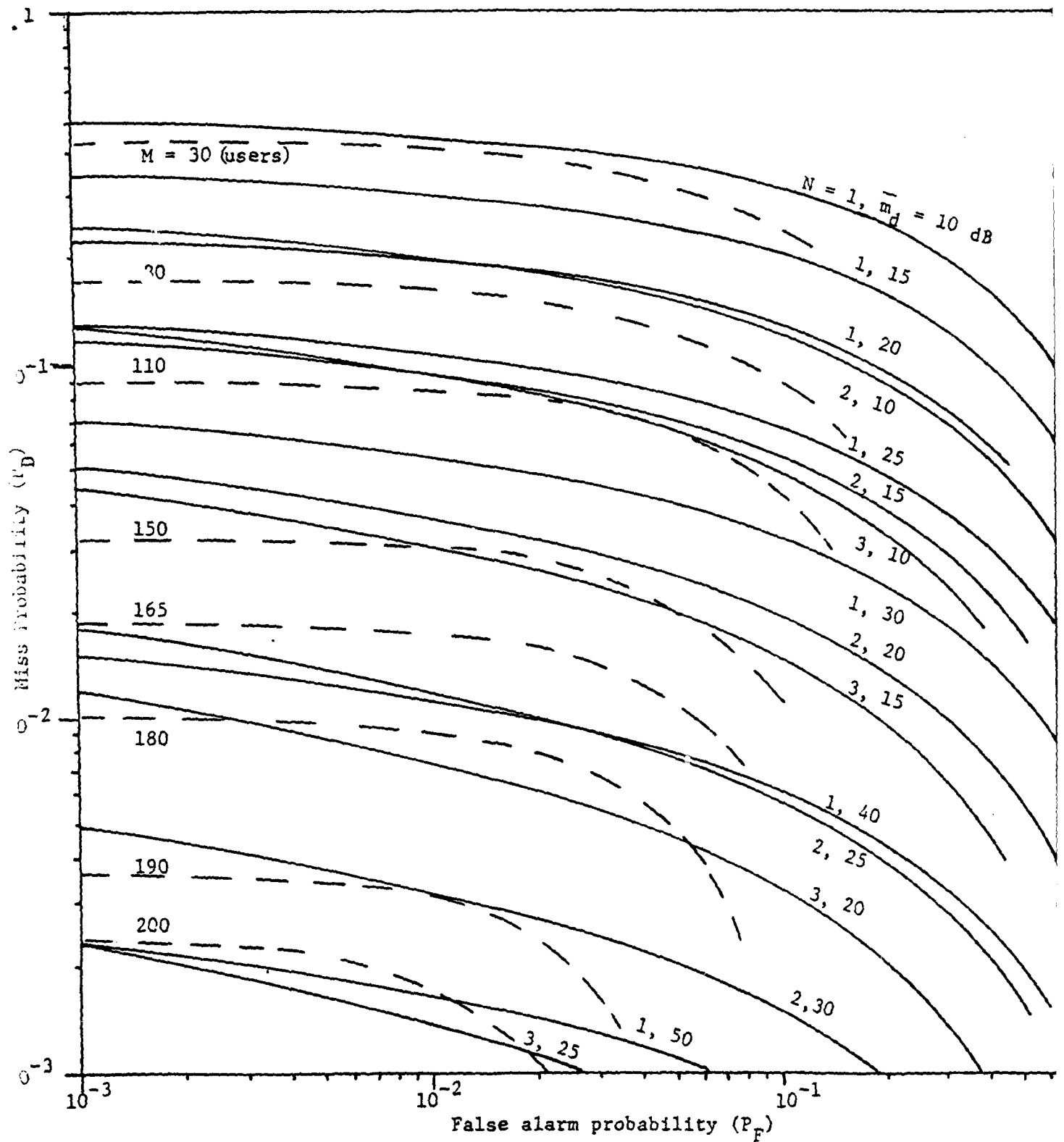
Figure 5-5 Constant M contour (broken) at an average bit error probability $P_B = 10^{-3}$

with $\hat{K} = 8$ and $\hat{L} = 19$. The receiver operation curve (solid) for $\sigma = 12$ d]

with N and $\bar{m}_d$ as parameters.
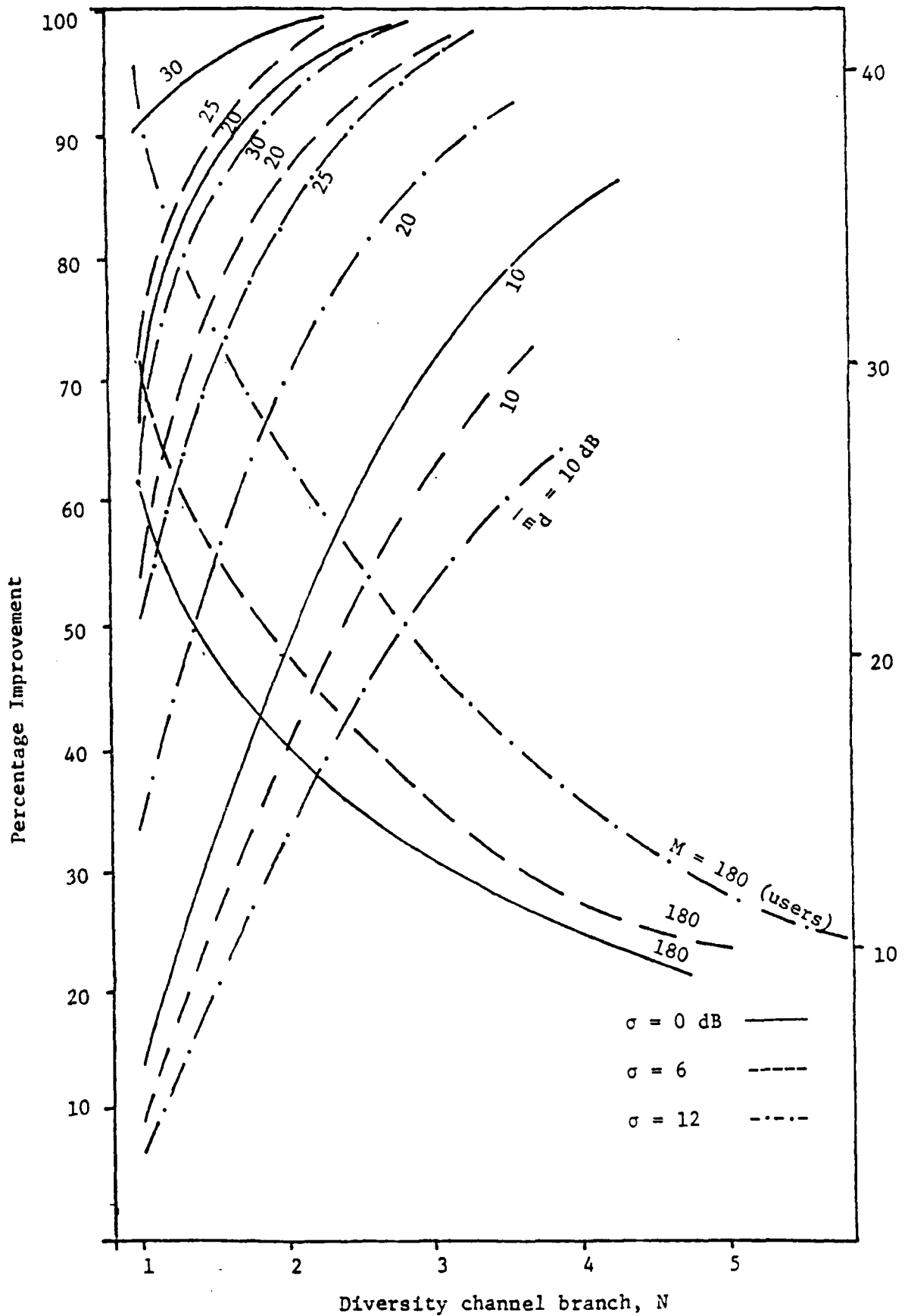
Fig. 5-6 The relative percentage improvement in system capacity and
the required $\gamma_o(\sigma = 0)$ or $\overline{m}_d(\sigma > 0)$ as a function of N with
$\overline{m}_{,,}$ $\sigma$ and M as parameters at $P_- = 10^{-3}$, W = 20 MHz
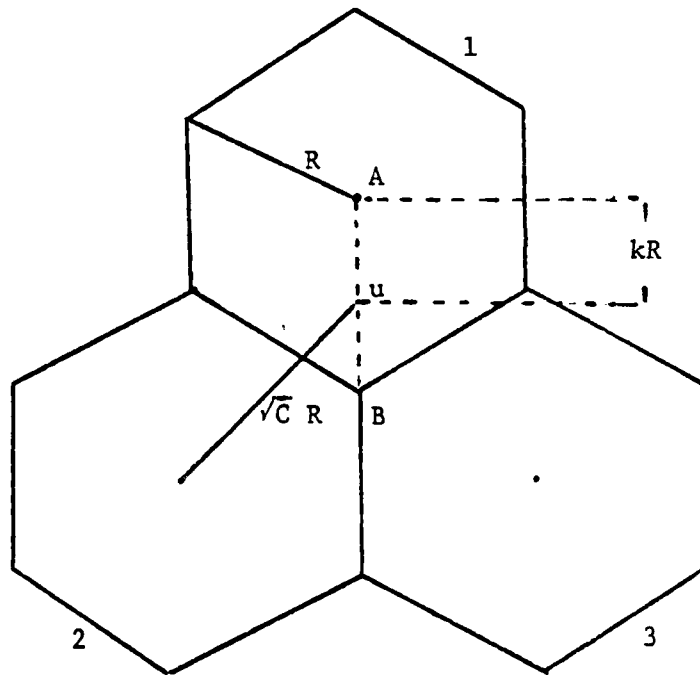
Figure 6-1   Three-cell Geometry
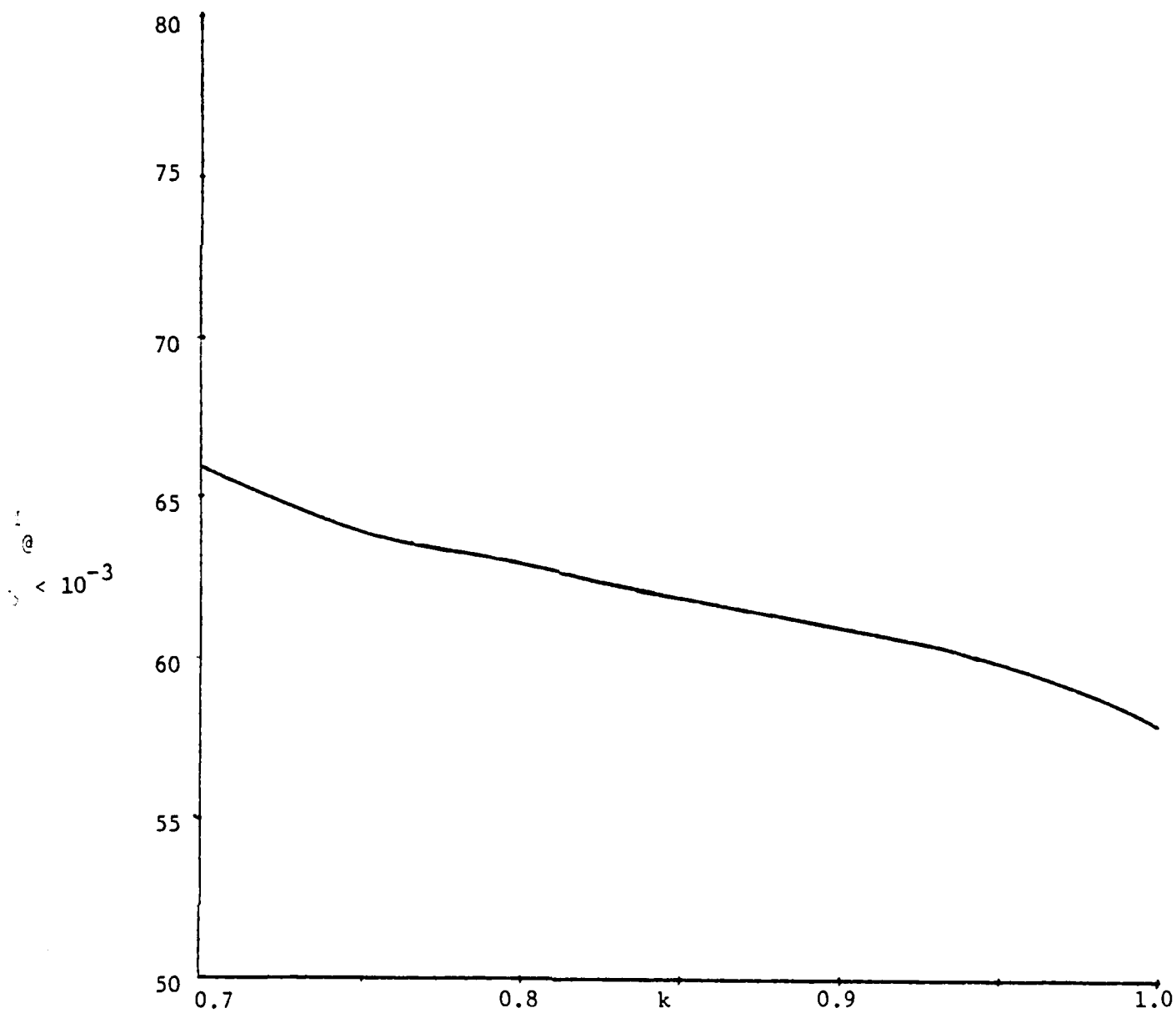
Fig. 6-2 Number of users at $P_b < 10^{-3}$ vs. distance of user u from base
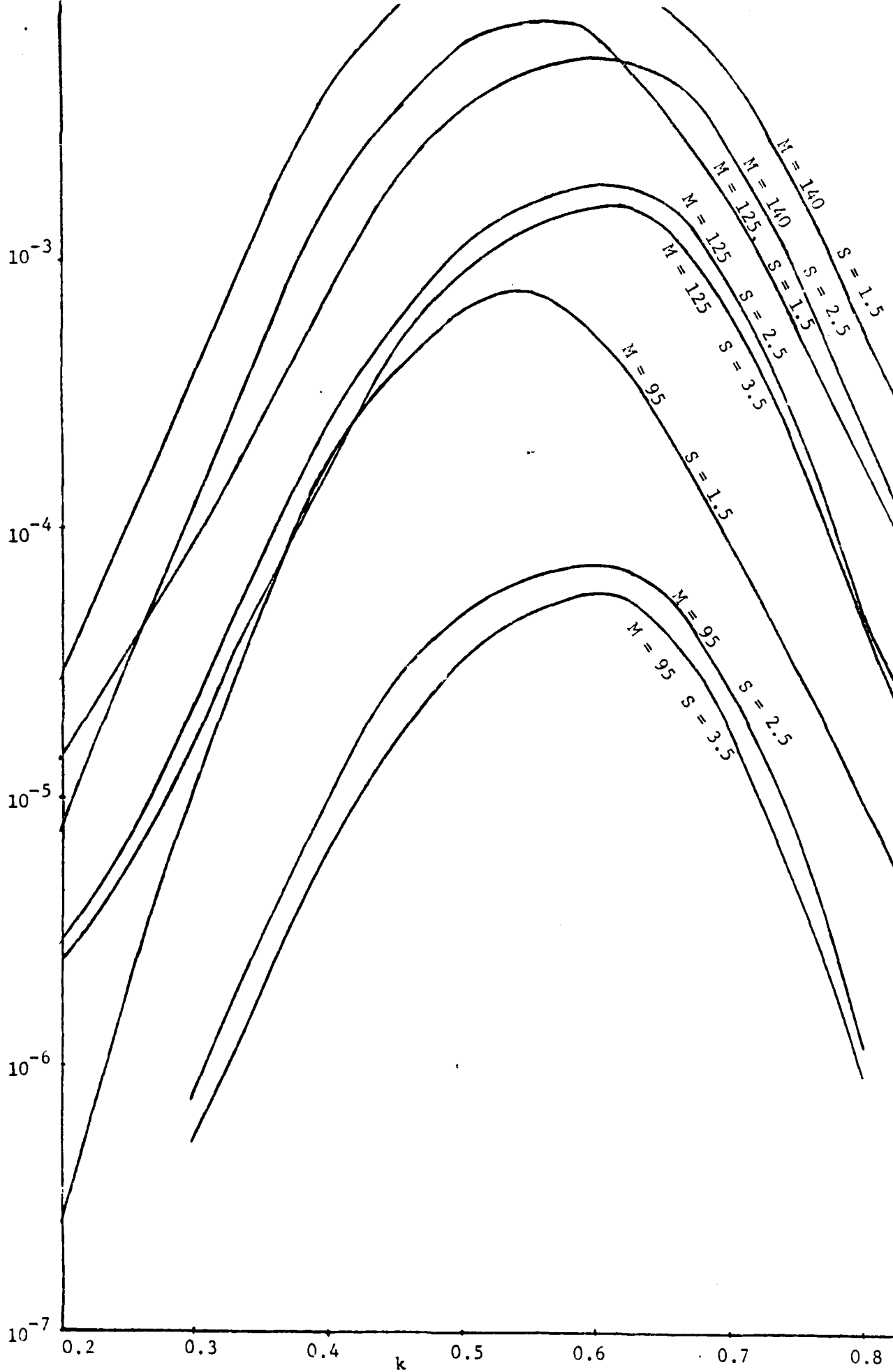
Figure 6-3 Probability of bit error vs. distance of user u from base 1.
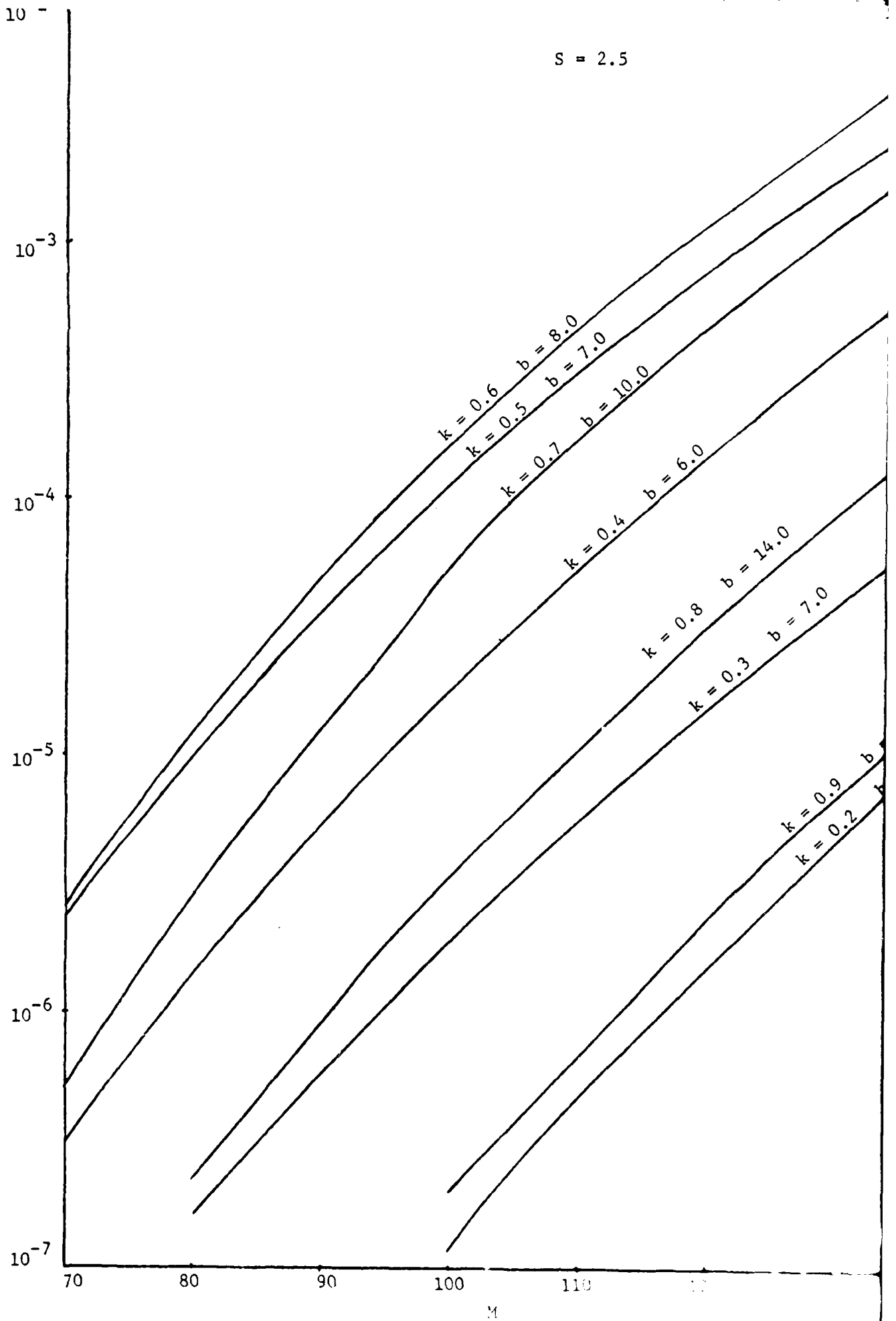
Figure 6-4 Probability of bit error vs. number of
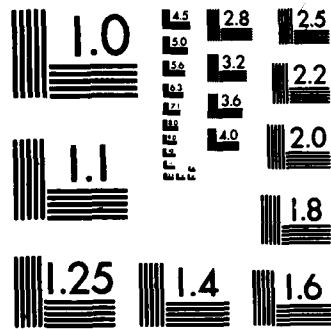
MICROCOPY RESOLUTION TEST CHART

NATIONAL BUREAU OF STANDARDS-1963-A
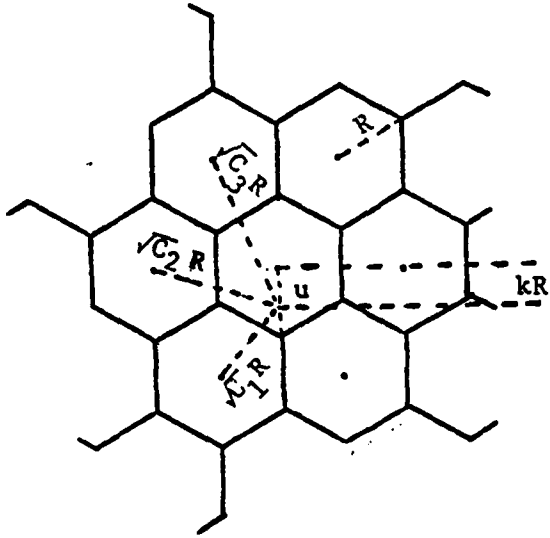
Figure 6-5 General cellular structure
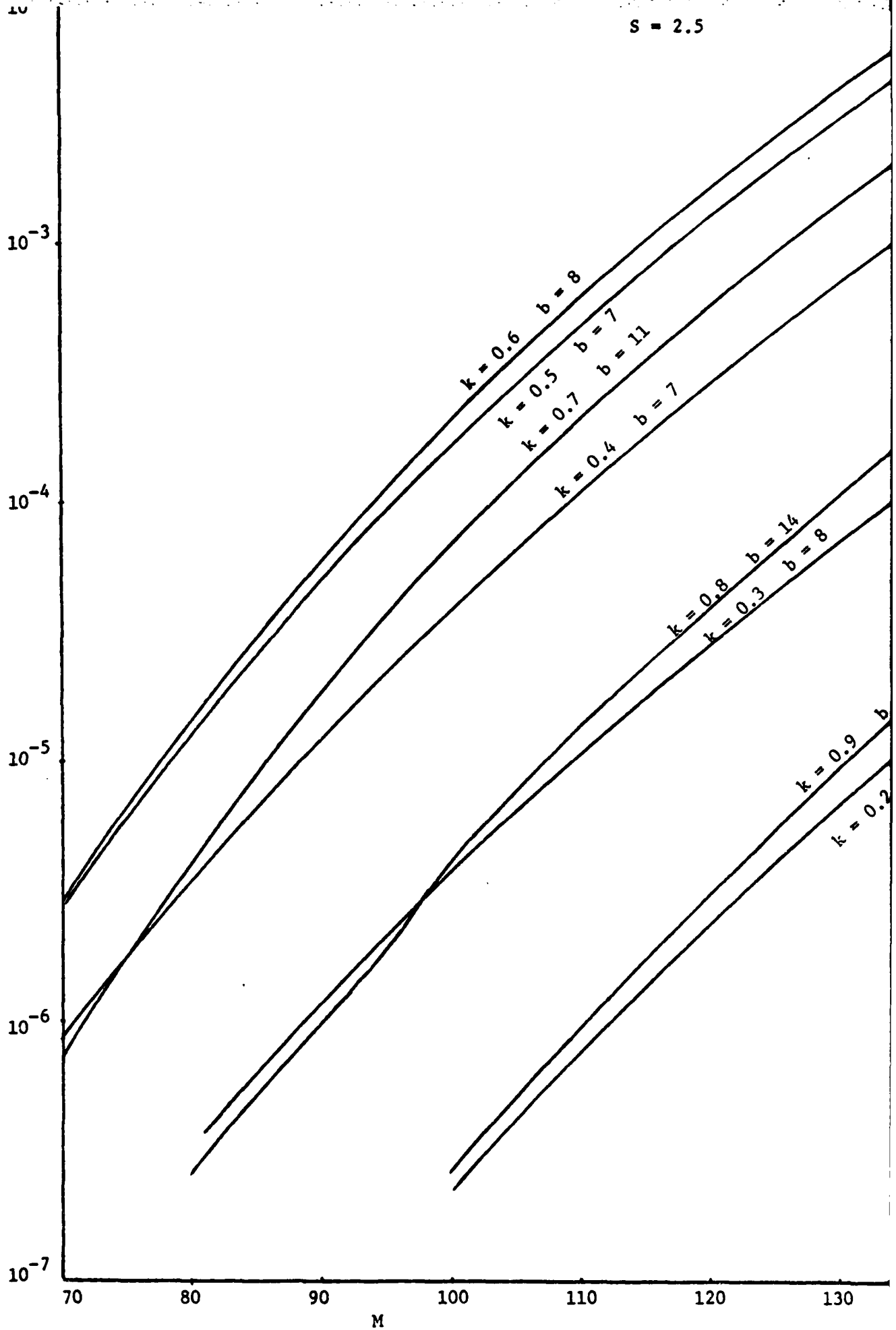
Figure 6-6 Probability of bit error vs. number of users in each cell.
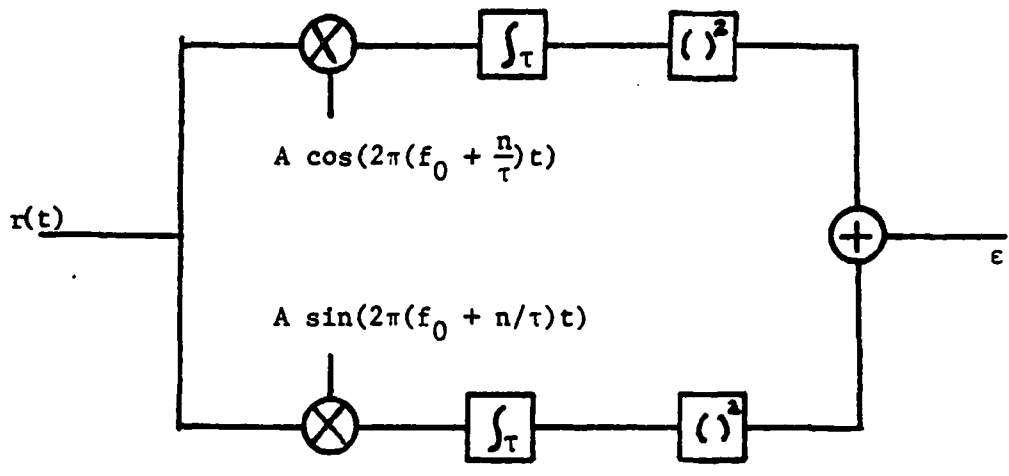
Figure 7-1    Envelope Analyzer
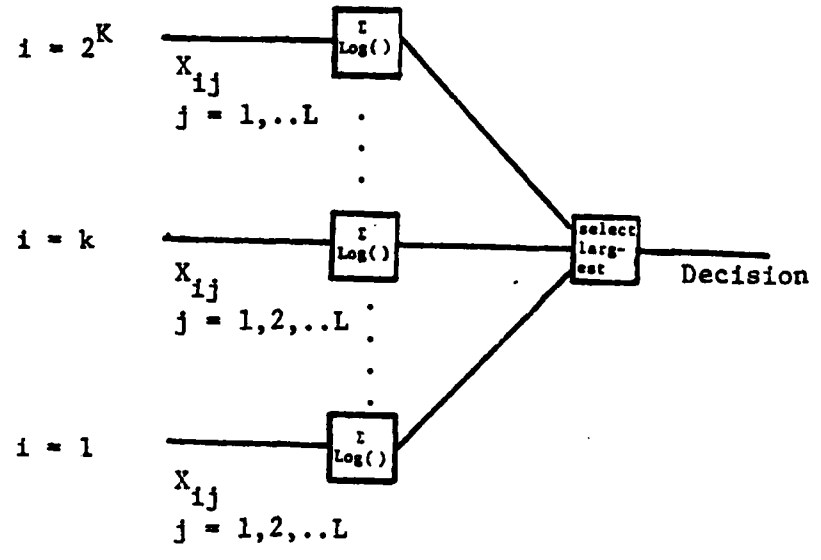


Figure 7-2    Likelihood Receiver
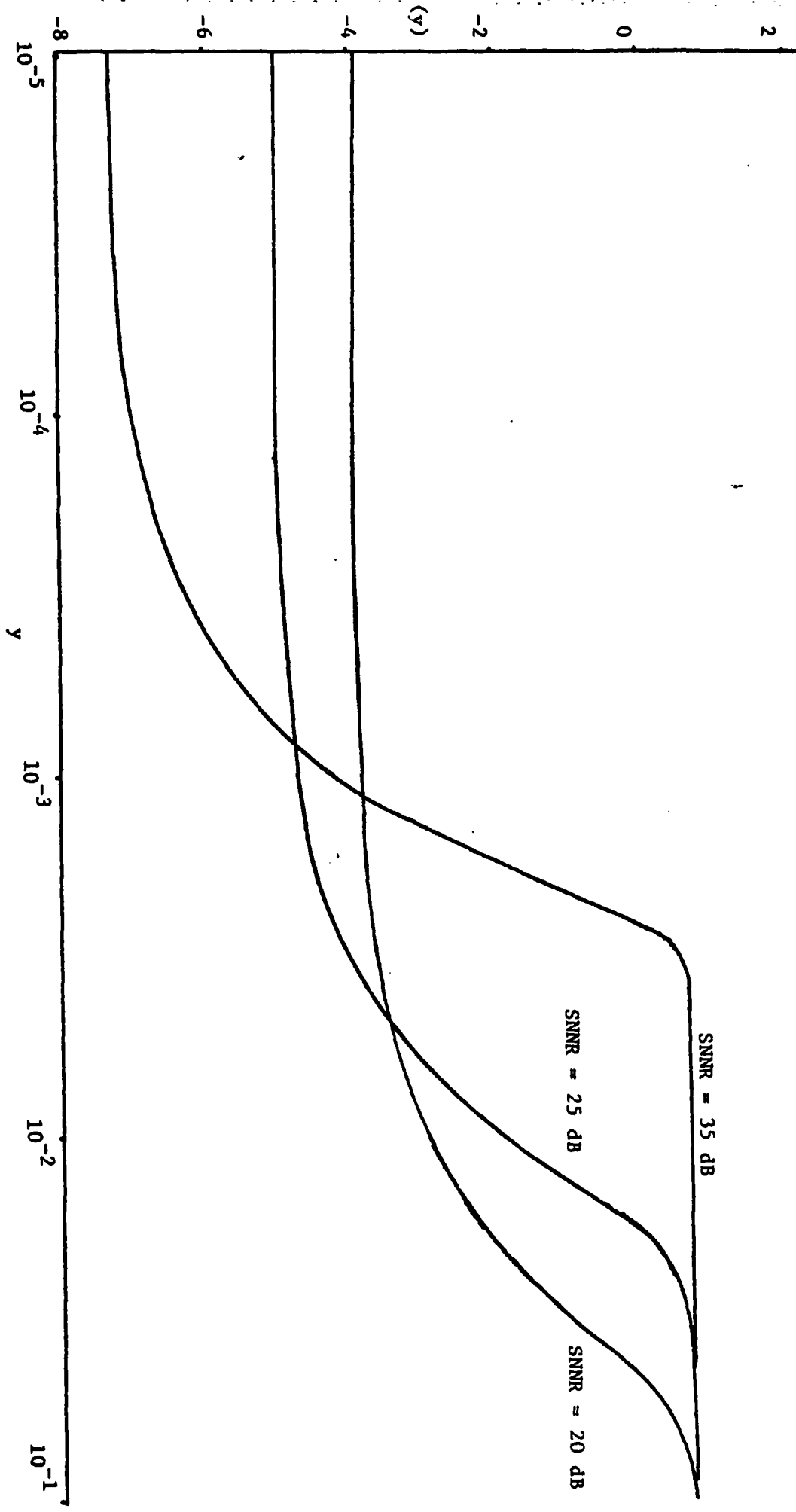
Figure 7-3  Plot of non-linearity

K = 8
L = 19

A    SNNR = 25 dB

A    SNNR = 35 dB
C

B    SNNR = 25 dB

D        C

B    SNNR = 35 dB

A: Chernoff Bound

B: C.B. with central lin
   theorem (or) one term
   saddle point approxim

C: Two term saddle point
   approximation

D: Asymptotic error rate
   (SNR → ∞)
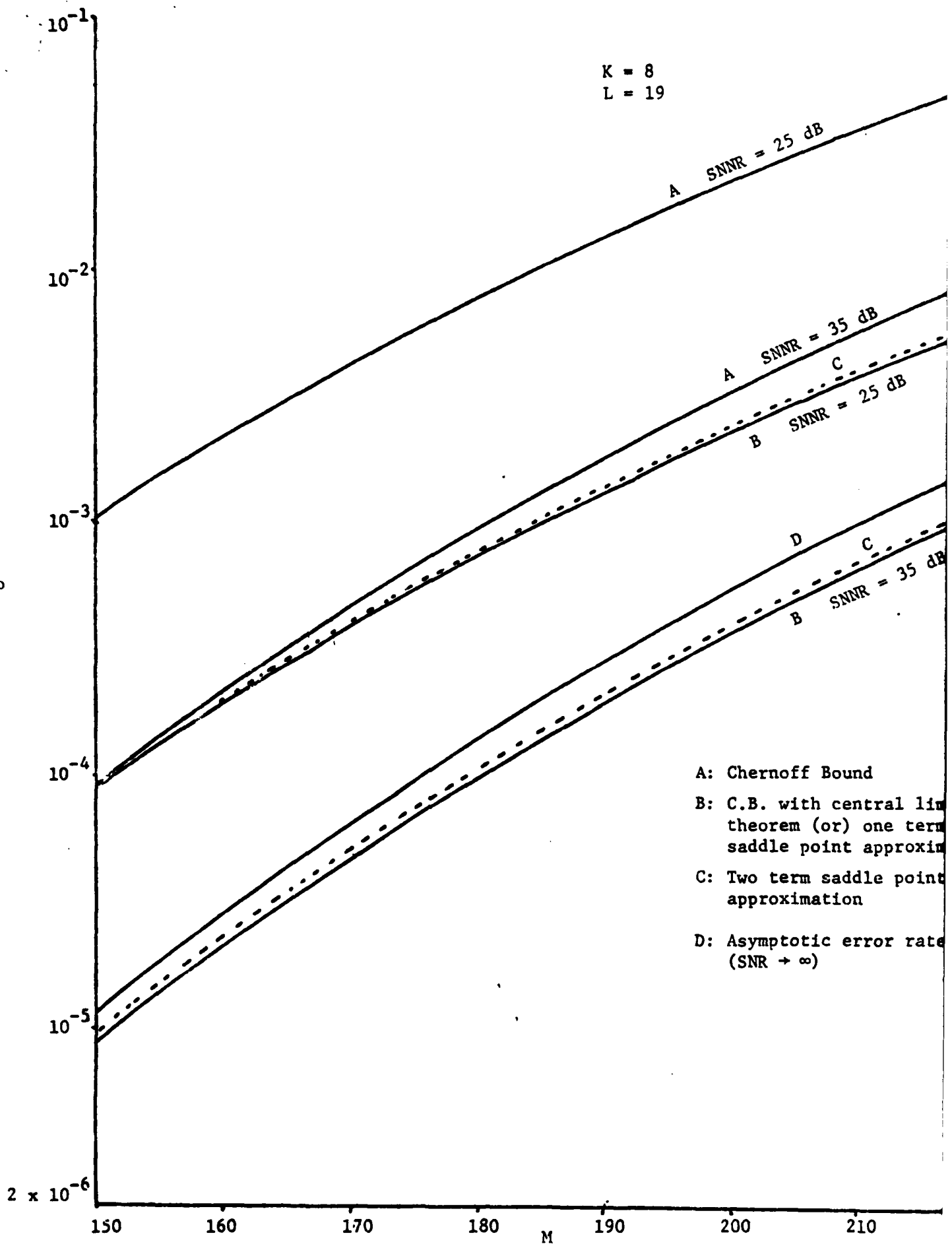
Figure 7-4 Probability of bit error vs. number of users for likelihood receiver
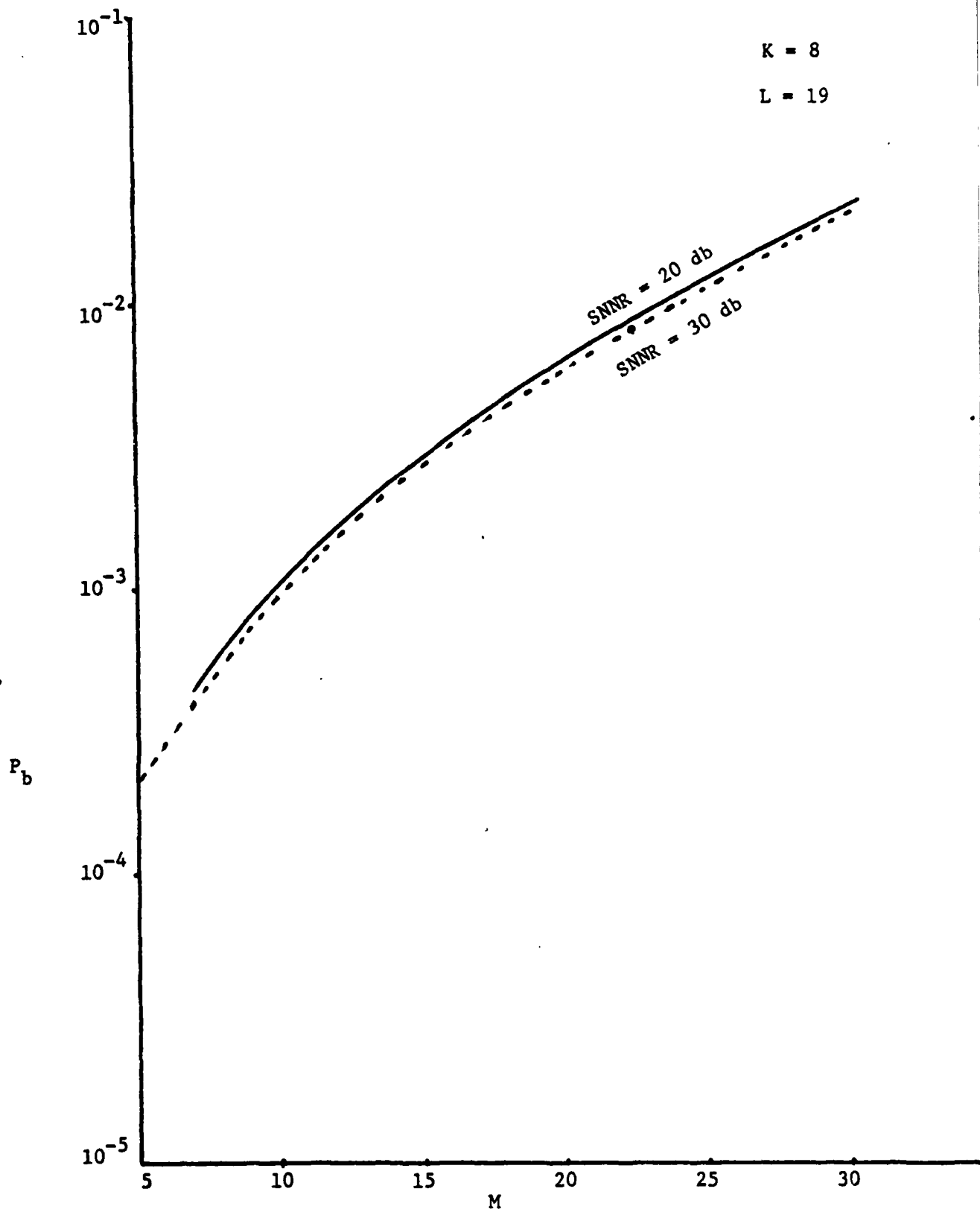
Figure 7-5   Probability of bit error vs. number of users for
             linear combiner.

5-83

DTIC